UDC 551.509.61:551.515.23

Analysis of Hurricane Debbie Modification Results Using the Variational Optimization Approach

ROBERT C. SHEETS—*National Hurricane Research Laboratory, NOAA, Miami, Fla.*

ABSTRACT—A variational optimization technique is used to develop an analysis scheme for application to the high energy portion of a hurricane. Derived analysis equations are used to filter the data in an attempt to obtain the signal for selected scales of motion. The selection of the particular filters used is based on empirical evidence. The analysis scheme is applied to data collected from airborne platforms in Hurricane Debbie of 1969 during two modification attempts. Results of these analyses are then used to define a more explicit seeding hypothesis, which can be used in the explanation and statistical evaluation of future seeding experiments. While it is felt that strong physical inferences can be drawn from the analysis results, more such data analyses are required before definitive statistical support can be claimed.

1. INTRODUCTION

Two basic questions must be answered in any attempt to determine possible effects of hurricane modification attempts. What changes in structure or intensity occur, and what, if any, portion of the observed changes result from the modification efforts? The analyses discussed in this paper attempt to provide answers for the first question and permit one to make strong inferences about the seeding effects.

Many factors concerning general or climatic conditions must also be considered. Several attempts have been made to provide background or climatic information about mean hurricane structure and natural diurnal variation (Jordan 1958, Sheets 1969*a*, 1970, 1972*a*, 1972*b*). In addition, several case studies of the structure of the high energy portion of the hurricane have been completed (Colon 1961, 1964, Hawkins and Rubsam 1968, LaSeur and Hawkins 1963, Sheets 1967*a*, 1967*b*, 1968). Most of these studies are based upon invaluable information collected onboard highly instrumented aircraft (Friedman et al. 1969*a*, 1969*b*), which have been monitoring the high energy portion of hurricanes over the past few years.

A variety of types, sizes, and strengths of hurricanes and their associated structures have been investigated. Although these storms exhibit structural differences, many common features are present. Pertinent to this study is the presence of small areas of extremum (maximum and minimum) values in the horizontal analyses of the various parameters such as wind speed, temperature, and moisture. Maximum centers are often associated with major rainbands or strong cells within the rainbands. These features are prominent in the middle and lower troposphere and apparently circulate, propagate, or form and dissipate around the storm center. This natural condition results in large fluctuations of a given parameter in both space and time. For instance, wind speed changes of as much as 20 to 30 percent over short time periods at a location fixed with respect to the storm center are not uncommon. Fluctuations of this same magnitude are observed over short horizontal distances in space. Both of these features are readily apparent in the analyses of Hurricane Dora on Sept. 7 and 8, 1964 (Sheets 1968). These fluctuations can easily mask changes in the mesoscale intensity or structure of the storm.

The results of the case studies previously mentioned show that a simple analysis of changes of the hurricane intensity could be misleading. This is especially true where no large statistical sample is available. These results further indicate that significant portions of the large, short time and space fluctuations are apparently associated with a few selected scales of motion. If this is true, then it seems necessary to determine what these scales are, their contributions to the total change, and their conservativeness from hour to hour, day to day, and storm to storm. Also, it would be desirable to determine whether or not these features are affected by specified types of modification attempts. Therefore, some filtering technique must be applied to data recorded in the hurricane to determine what portion of the total signal resulted from a particular feature. For instance, what portion of the total wind speed recorded within a cumulonimbus cloud embedded in a rainband resulted from the presence of the cloud? Likewise, what portion resulted from the presence of the rainband?

Standard filtering techniques are difficult to apply because the overwhelming percentage of the variance is contained in the longer wavelength features. Data records of unequal length, large variations in endpoint values, and mispositioned data also present problems. Many of the more refined techniques become complicated and require a considerable number of fixed endpoint values. The variational optimization approach offers a method for obtaining nearly the same information with much less difficulty. Therefore, this approach was chosen for the analyses presented in this paper.

The filtered data are stratified according to the scale of motion. An attempt is made to determine if an organized sequence of changes exists, (e.g., from small scales to larger scales). Particular emphasis is placed on determining this sequence since it is improbable that enough seeding cases will be available in the near future for application of standard statistical tests. This approach should also aid in the development of a more explicit seeding hypothesis.

2. HURRICANE DEBBIE (1969) SEEDING EXPERIMENTS AND RELEVANT HYPOTHESES

Rosenthal (1971) has provided an excellent historical review and interpretation of the development and evolution of hurricane eyewall seeding hypotheses. Selected excerpts of the report are repeated here, but it is recommended that the reader refer to sections 4 and 5 of the referenced report to obtain a more complete understanding of the "seeding hypothesis evolution."

Many studies have shown that the hurricane eyewall cloud is generally located in the region of maximum low-level pressure gradient. Early investigators believed that these wall clouds contained significant quantities of supercooled water. This belief was substantiated by observations from flights at altitudes above the freezing level and was verified in recent investigations (Sheets 1969*b*). These facts led Simpson and Malkus (1964) to propose an eyewall seeding hypothesis. This hypothesis (referenced as hypothesis I) is paraphrased by Rosenthal (1971) as follows:

"If this supercooled water were frozen through nucleation by silver iodide crystals, the released heat of fusion would produce temperature increases; and therefore, hydrostatically, pressure decreases near the region of the strongest pressure gradient. If the central pressure did not concomitantly decrease, a reduction in maximum pressure gradient, and in turn, a reduction in wind speed should be the net result."

[The increase in temperature due to the directly released heat of fusion is actually a relatively small part of the total process ($\approx$80 cal/g). The major change resulting from the freezing of the supercooled water, of course, is the enhancement of the natural processes of ice crystal growth and splintering, providing many more freezing nuclei. This process results in a rapid increase in the rate of release of latent heat of sublimation and fusion ($\approx$680 cal/g).]

Rosenthal then offered several arguments indicating a necessary modification of the hypothesis and the design of the experiments to attain the desired results. The most significant of these arguments is "the fact that the eyewall drives the storm's transverse circulation and seeding this region alone would very likely accelerate this circulation thus providing a more rapid inflow of both angular momentum and water vapor to the eyewall region."

Rosenthal performed several simulated seeding experiments with his numerical hurricane model. The results of these experiments and the physical arguments against hypothesis I led him and others associated with project Stormfury to propose a different hypothesis as follows:

"Hypothesis II differs from Hypothesis I in that the latter calls for seeding the eyewall alone whereas the former suggests seeding either from the eyewall outward or entirely outward from the eyewall. While the logistics of these hypotheses differ only slightly, the physical arguments are substantially different. In Hypothesis II, the basic idea is to stimulate convection and ascent at radii greater than that of the eyewall. The region of stimulated convection is intended to compete with the eyewall for the inflowing air at low levels. If significant portions of the inflow can be diverted upward at the seeded radii, the angular momentum and water vapor supplies to the original eyewall and wind maximum will be reduced. As a consequence, one would expect the original wind maximum to be reduced and the eyewall convection to be diminished."

Calculations by the author (Sheets 1969*c*) indicate that it is difficult to get much more vertical growth of the hurricane eyewall cloud by seeding. This is a result of the neutral stability condition caused by the release of latent heat at the upper levels. However, as one proceeds outward from the eyewall, the potential for increased growth of clouds extending above the freezing level and containing supercooled water increases markedly. This fact, along with the knowledge of the presence of the required supercooled water in the clouds outside the eyewall (Sheets 1969*b*), offers further evidence supporting the potential of hypothesis II.

The hurricane Debbie experiments carried out on August 18 and 20 of 1969 were performed in the manner suggested by hypothesis II. These experiments are described in considerable detail by Gentry (1970). Only those portions directly related to the analysis in this paper are given here. Figure 1 shows the track and geographical locations of the storm during the two experiments. Figure 2 shows the pattern of the seeding track. Five seeding runs were made at approximately 2-hr intervals during each of the two seeding experiments. Figure 3 shows the flight tracks of the National Oceanic and Atmospheric Administration (NOAA) Research Flight Facility DC–6 aircraft. The analyses performed in this paper are based on the data obtained during these missions.

There were three monitoring flights at the 12,000-ft level for each of the two experiments. The pattern basically consisted of two traverses through the center of the storm along the direction of motion and then repetitive traverses normal to the axis of the storm movement for the remainder of the flight. The monitoring missions began some 2 hr prior to the first seeding run and lasted some 4–6 hr after the final seeding event.

Measurements of the standard meteorological parameters were digitally recorded on magnetic tape at 1-s intervals (Friedman et al. 1969*b*). These data then went through a rigorous processing procedure where the winds, aircraft position, and other data were recomputed from the raw data recorded on the original tape. This procedure included calibration of the signals recorded from several instruments. These processed data were then averaged

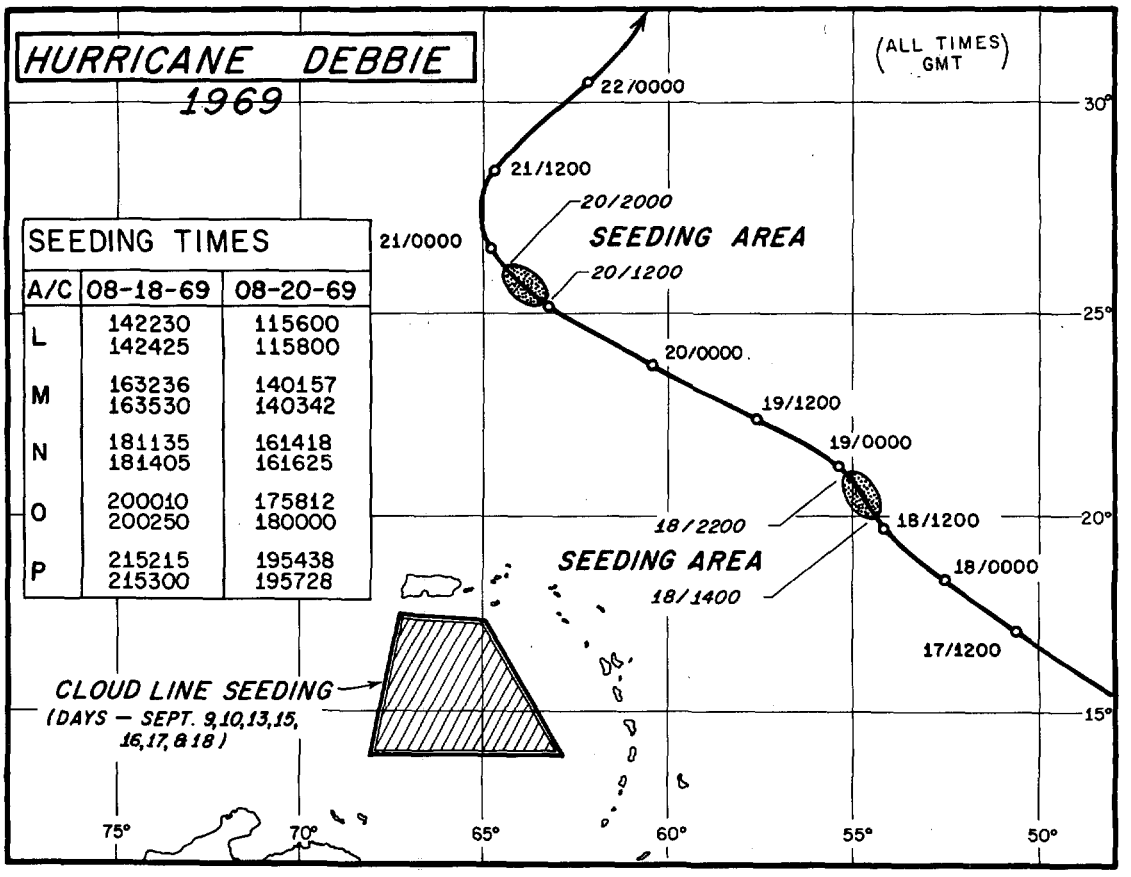

SEEDING TIMES		
A/C	08-18-69	08-20-69
L	142230 142425	115600 115800
M	163236 163530	140157 140342
N	181135 181405	161418 161625
O	200010 200250	175812 180000
P	215215 215300	195438 195728

FIGURE 1.—Hurricane Debbie of 1969 storm track and geographical locations of the modification experiments.

over 1-n.mi. radial distance intervals from the storm center for input into the analysis scheme developed in the next section.

3. DEVELOPMENT OF THE ANALYSIS EQUATION

The variational optimization technique (Sasaki 1958, 1968, 1970*a*, 1070*b*, 1970*c*) is used in this paper as a means of filtering and for developing a more explicit seeding hypothesis. The method is based on a functional that defines selected optimization constraints. The functional, J_1, consists of two low-pass filters with an "observational constraint."

The functional is defined as follows:

$$J_1=\sum_r\left[\beta\left(\frac{\partial^2\theta}{\partial r^2}\right)^2+\gamma\left(\frac{\partial\theta}{\partial r}\right)^2+\alpha(\theta-\tilde{\theta})^2\right]dr, \qquad (1)$$

where θ is the analyzed value of any variable, $\tilde{\theta}$ is the observed value of the variable θ, and r is radial distance from the hurricane center. The first two terms act as low-pass filters and the last term is similar to a "least-square-fitting" of the derived field to the observations (Wagner 1971). These three terms will be referred to in the remainder of this paper as the *curvature*, *gradient*, and *observational* constraints, respectively. The quantities α, γ, and β are the weights placed on these respective terms and, as will be shown later, determine the degree of filtering imposed on the analyses.

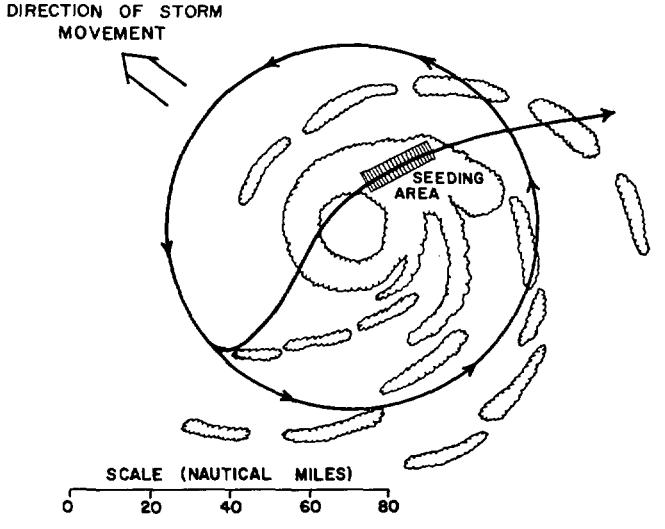

FIGURE 2.—Seeding area and flight pattern (altitude 33,000 ft) for the seeder aircraft.

The nondimensional finite-difference analog for eq (1) (Sheets 1973) becomes

$$J_1=\sum_r[\beta(\nabla_r^2\theta)^2+\gamma(\nabla_r\theta)^2+\alpha(\theta-\tilde{\theta})^2]\Delta r. \qquad (2)$$

All terms are quadratic. Therefore, the minimum value of the functional will be obtained by taking the first variation (similar to differentation) of eq (2) with respect

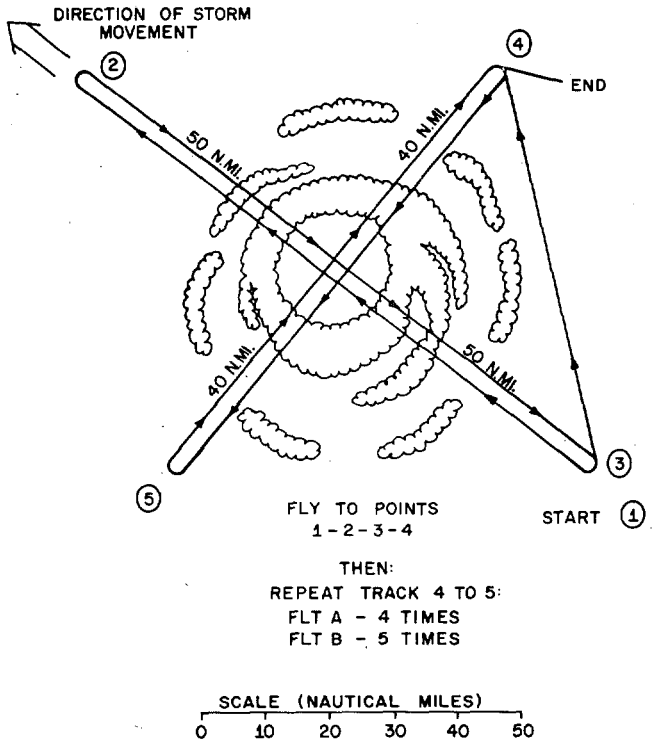

FIGURE 3.—Flight pattern (altitude 12,000 ft) for NOAA Research Flight Facility DC-6 aircraft eyewall experiment monitoring missions.

to θ and letting the first variation vanish under the proper boundary condition.

Applying rules of variational calculus and taking the first variation of eq (2) with respect to θ, we obtain

$$\delta_\theta J_1=\sum_r \{2\beta(\nabla_r^2\theta)\,[\nabla_r^2(\delta\theta)]+2\gamma(\nabla_r\theta)[\nabla_r(\delta\theta)] +2\alpha(\theta-\tilde{\theta})\delta\theta\}\nabla r=0. \quad (3)$$

We now use summation by parts and assume natural boundary conditions (Sasaki 1969). Therefore, eq (3) becomes

$$\delta_\theta J_1=\sum_r \{[2\beta\nabla_r^4\theta-2\gamma\nabla_r^2\theta+2\alpha(\theta-\tilde{\theta})]\,\delta\theta\}\Delta r=0. \quad (4)$$

Since the variation, $\delta\theta$, is arbitrary, eq (4) implies that

$$\beta\nabla_r^4\theta-\gamma\nabla_r^2\theta+\alpha(\theta-\tilde{\theta})=0 \quad (5)$$

which is the classical Euler-Lagrange or Euler equation and also is referred to as the analysis equation in Sasaki's method of variational analysis. This equation is readily solved by standard iterative techniques. The Liebmann method was used for this paper.

Response Function

The response function for the finite-difference analog of the analysis equation [eq (5)] is derived to determine the desired values for the weights α, γ, and β. The n components of the "true" and analyzed field, $\tilde{\theta}_n$ and θ_n, respectively, are assumed to be represented by

$$\tilde{\theta}_n=Ae^{ikn\Delta r}$$

and (6)

$$\theta_n=Be^{ikn\Delta r}$$

where k is the wave number and A and B are constants.

Substituting eq (6) into (5) we obtain

$$\frac{Be^{ikn\Delta r}}{Ae^{ikn\Delta r}}=\alpha\left[\alpha-\frac{\gamma(2\cos k\Delta r-2)}{\Delta r^2}+\frac{\beta(2\cos 2k\Delta r-8\cos k\Delta r+6)}{\Delta r^4}\right]^{-1}.$$

Defining the response function, R, to be the ratio of the analyzed value to the true value results in

$$R=\frac{\theta}{\tilde{\theta}}=\left[1-\frac{2\gamma(\cos k\Delta r-1)}{\alpha\Delta r^2}+\frac{2\beta(\cos 2k\Delta r-4\cos k\Delta r+3)}{\alpha\Delta r^4}\right]^{-1}. \quad (7)$$

The wavelength, L, is expressed in multiples of the grid size. Using the factor k/k_0, where k_0 is some characteristic wave number ($2\pi/100$ n.mi. in this paper) and P is defined as the number of grid intervals per wavelength; that is,

$$P=\frac{L}{\Delta r},$$

$$k_0=\frac{2\pi}{100\text{ n.mi.}},$$

$$\frac{k}{k_0}=\frac{100}{L},$$

or

$$L=100\left(\frac{k_0}{k}\right),$$

and $\Delta r=1$ n.mi. or finally,

$$P=\frac{100}{\frac{k}{k_0}},$$

we obtain

$$R=\left\{1-\frac{\alpha k_0^2(100)^2}{\gamma 2\pi^2}\left[\cos\left(\frac{2\pi\frac{k}{k_0}}{100}\right)-1\right]+\frac{\beta k_0^2(100)}{\gamma 32\pi^4}\left[\cos\left(\frac{4\pi\frac{k}{k_0}}{100}\right)-4\cos\left(\frac{2\pi\frac{k}{k_0}}{100}\right)+3\right]\right\}^{-1}. \quad (8)$$

Figure 4 illustrates this response factor plotted as a function of the wavelength and for selected values of the weights α, γ, and β. Figure 4 also illustrates the difference between selected low-pass filter response curves. In some cases, the resulting difference has been amplified to make the peak response value equal to 1. These low-pass and band-pass filters are used extensively in the analysis portion of this paper. They will be referred to as filters A,

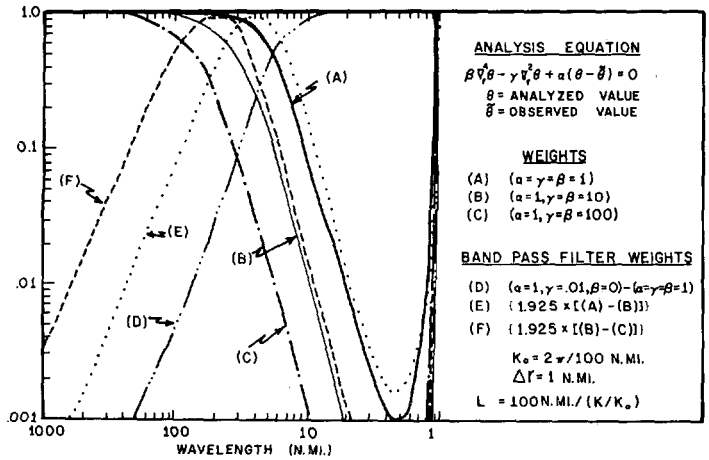

FIGURE 4.—Response curves for the analysis equation derived from the functional J_1 for selected weights.

B, and C, and band filters D, E, and F, corresponding to their designation in figure 4.

Selection of the values for the weights α, γ, and β was based on empirical evidence. As was discussed in the introduction, we wish to examine separately and in detail the response from prominent individual features in the hurricane such as cumulonimbus clouds, rainbands, and the eyewall as well as the mesoscale features. Therefore, the weights used in the design of filter A were chosen so that the contributions to the total signal for a given parameter from cumulonimbus and smaller scale motions are removed. That is, when filter A is applied to a given set of data, only that portion of the signal resulting from scales of motion greater than approximately 10 n.mi. in wavelength are retained. This degree of filtering was obtained by applying equal weight on the observational and low-pass filter terms. To obtain only that portion of the signal associated with the cumulonimbus and smaller scale features, one simply takes the difference between the original data values and those obtained by application of filter A. These results, then, basically correspond to the results obtained by application of filter D and are illustrated in figure 7.

The weights used in the design of filter B were chosen so that only approximate eyewall and larger scale motions were retained. This degree of filtering was obtained by placing greater weights on the low-pass filter terms than were used for filter A. If one takes the difference between the values obtained by applications of filter A and filter B, the results correspond to the signal obtained from approximate rainband-scale motion. These results, along with an amplification factor, correspond to values obtained by application of band filter E. This band filter is centered at a wavelength of 25 n.mi. where 100 percent of the signal for this scale of motion is obtained. The response then decreases for smaller and larger scale features becoming 50 percent at wavelengths of 15 and 50 n.mi. The results obtained from application of this band filter are referred to as approximate rainband-scale motion in the remainder of this paper.

The weights used in the design of filter C were chosen so that only the meso- and larger scale features were retained. That is, the weights applied to the low-pass filter terms were 10 times larger than the corresponding weights used for filter B. Again, taking the difference between the values obtained by applications of filters B and C corresponds to the response obtained from approximate eyewall-scale motion (band filter F). The results obtained in this manner, along with an amplification factor, are referred to as eyewall-scale motion and represent 100 percent of the response for 50-n.mi. wavelength features and decrease to 50-percent response at 30- and 100-n.mi. wavelengths.

The physical effect of the application of these filters to the observed data is somewhat analogous to the use of weighted centered averages. That is, the analyzed value for any gridpoint would be obtained by taking a weighted average of the observed values at and around the particular point with the greatest weight applied to the value at the central point. Filters A and C would correspond to averaging over a small and large distance, respectively. Therefore, the analyses resulting from application of filter C would be considerably smoother than those obtained by use of filter A.

4. ANALYSIS OF HURRICANE DEBBIE AUGUST 18, 1969

The method of analysis described in section 2 is applied to the data collected in hurricane Debbie on Aug. 18, 1969. These data were recorded aboard the NOAA DC–6 aircraft and were processed in the manner described in section 2. The variables investigated are wind, temperature, moisture, and pressure. The data are assumed to be collected instantaneously on a given pass. In actuality, the time required for the aircraft to make a single pass through the storm is approximately 20–30 min. These data are then averaged over small space and time intervals for each pass for insertion into the analysis equations. Each pass was then analyzed separately with the analysis equation being solved simultaneously for the entire pass. The grid interval chosen for the analysis was 1 n.mi.

Kinetic Energy

The application of filters A, B, and C shows large changes in the kinetic energy during the seeding experiment. The profiles shown in figure 5 are for prior to seeding, immediately after the third seeding run, and finally, about 4 hr after the final seeding event for the left and right sides of the storm. These profiles exhibit a large decrease in the maximum value of the kinetic energy for the sum of all wavelengths represented (i.e., A $\geq$ 10 n.mi., B $\geq$ 30 n.mi., C $\geq$ 80 n.mi.). This total decrease amounted to approximately 40 percent for each filtered quantity for the northeast or right side of the storm. The left side shows a net decrease in the maximum value of 31 and 18 percent for the kinetic energy in the wavelengths represented by A and B, respectively, but

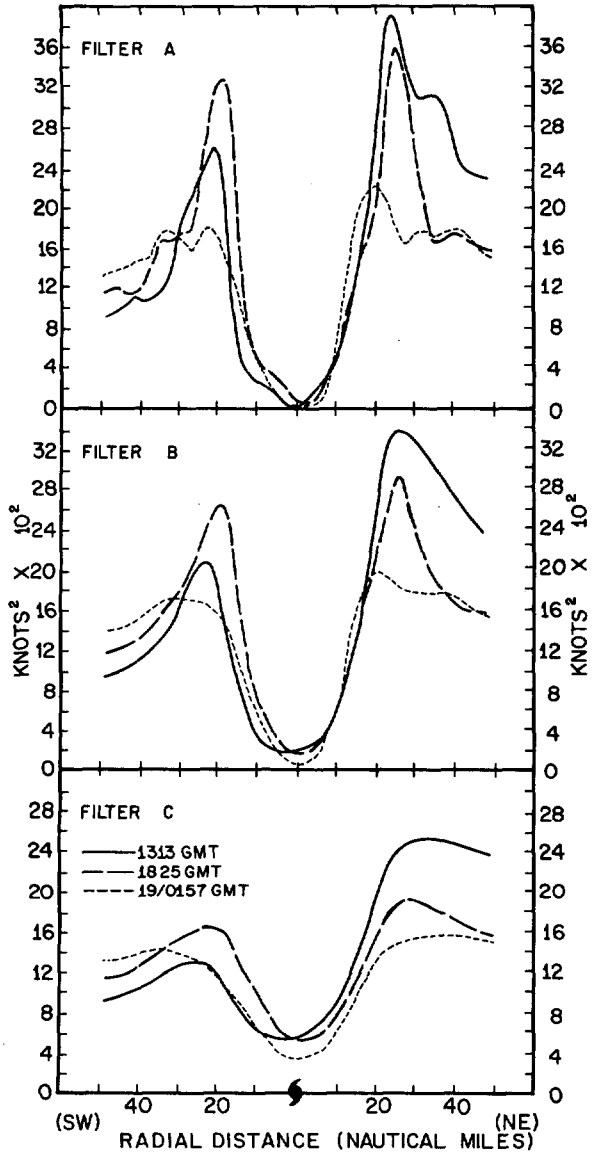

FIGURE 5.—Kinetic energy profiles for the left and right (SW–NE) sides of hurricane Debbie, obtained by application of filters A, B, and C to observed data for Aug. 18, 1969.

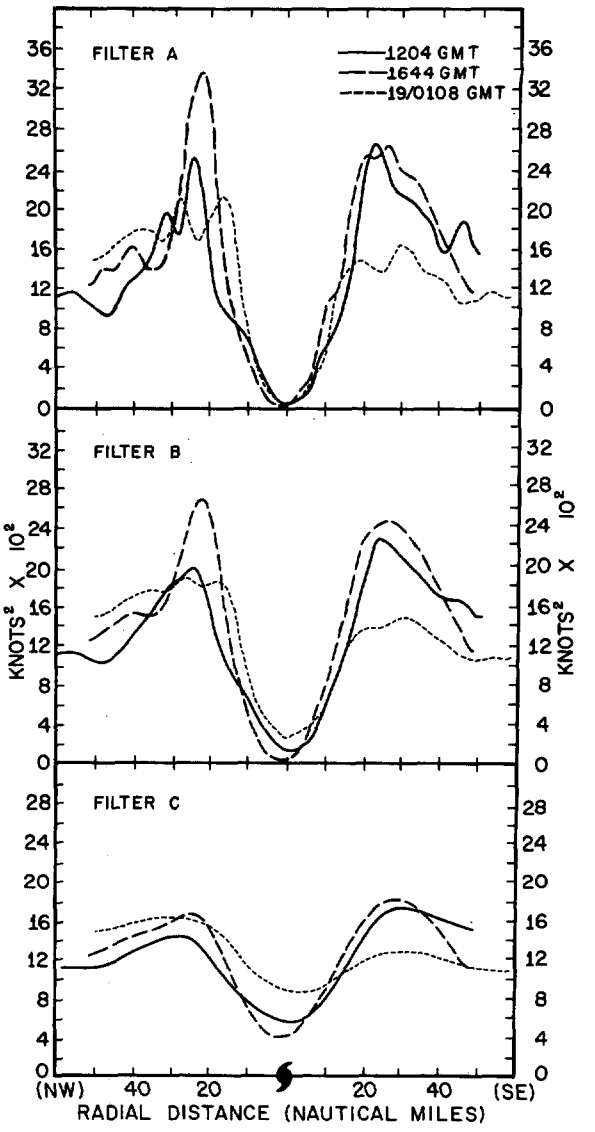

FIGURE 6.—Same as figure 5 for the front and rear (NW–SE) portions of the storm.

a net increase of 9 percent for those wavelengths associated with filter C. The southwest or left side of the storm also shows an increase in kinetic energy with time for larger radial distances from the storm center. The profiles of kinetic energy associated with these same filters for the northwest and southeast quadrants are shown in figure 6. The changes for the southeast quadrant range from 25- to 38-percent decreases for the three filtered quantities (table 1), while a 15-percent decrease for filter A, 4 percent for filter B, and a 14-percent increase for filter C are shown for the northwest quadrant.

Of particular interest is the fact that, except for the southeast quadrant, approximately two-thirds of the total change that occurs in the longer wavelengths (filter C) has occurred by the time of the third seeding. The net change of the maximum value of kinetic energy for this same time period associated with filters A and B is considerably less. In fact, the changes in specific kinetic energy associated with filters A, B, and C for this

TABLE 1.—*Maximum (peak) values of the specific kinetic energy (Kt^2) and percent changes for each quadrant in hurricane Debbie on Aug. 18, 1969**

Filter	Obs. time (GMT) (SW–NE/SE–NW)	Quadrant SW	NE	SE	NW	Net
A	(1) 1313/1204	2604	3878	2625	2475	3878
	(2) 1825/1644	3248	3537	2610	3328	3537
	(3) 0157/0108	1789	2168	1613	2111	2168
	% change (1) to (2)	+24.73	− 8.79	− 0.57	+34.46	− 8.79
	% change (2) to (3)	−44.91	−38.70	−38.19	−36.56	−38.70
	% change (1) to (3)	−31.29	−44.09	−38.55	−14.70	−44.09
B	(1) 1313/1204	2049	3370	2251	1953	3370
	(2) 1825/1644	2620	2891	2438	2661	2891
	(3) 0157/0108	1667	1949	1486	1869	1949
	% change (1) to (2)	+27.86	−14.21	+ 8.30	+36.25	−14.21
	% change (2) to (3)	−36.37	−32.58	−39.04	−29.76	−32.58
	% change (1) to (3)	−18.64	−42.16	−33.98	− 4.30	−42.16
C	(1) 1313/1204	1307	2557	1712	1432	2557
	(2) 1825/1644	1664	1917	1811	1663	1917
	(3) 0157/0108	1423	1564	1291	1637	1637
	% change (1) to (2)	+27.31	−25.02	+ 5.78	+16.13	−25.02
	% change (2) to (3)	−14.48	−18.41	−28.71	− 1.56	−14.60
	% change (1) to (3)	+ 8.87	−38.83	−24.59	+14.31	−35.97

*These values were obtained by application of filters A, B, and C and are given by quadrant as well as the net change regardless of quadrant.

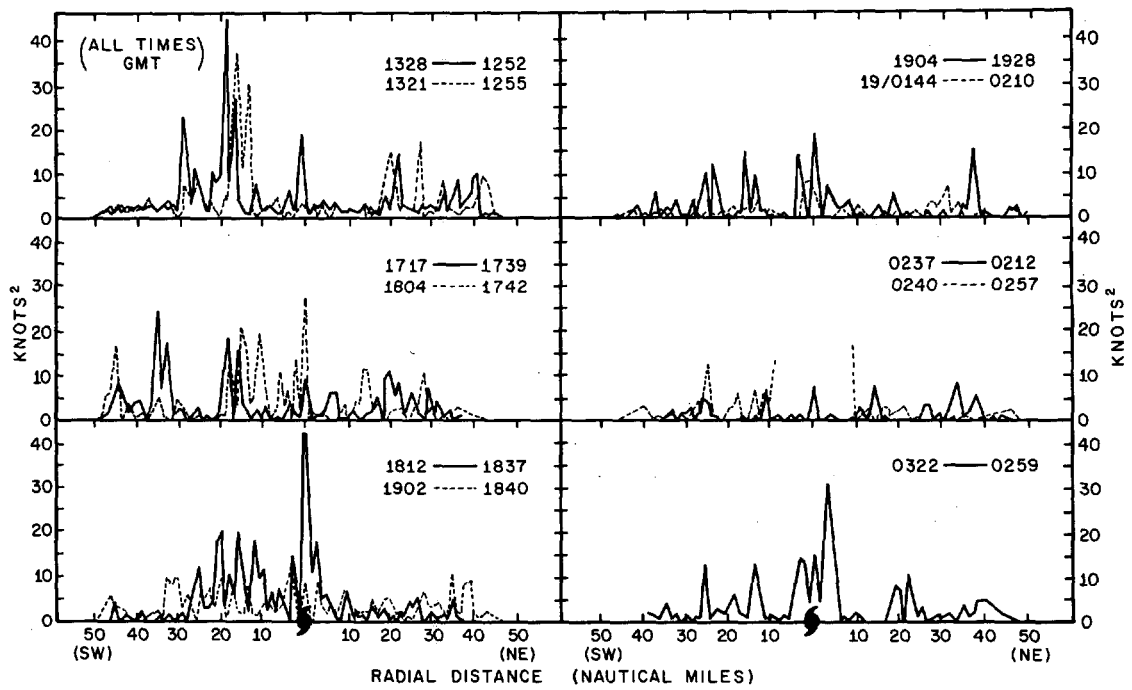

FIGURE 7.—Kinetic energy profiles for the left and right (SW–NE) sides of hurricane Debbie resulting from application of band filter D (≈ cumulonimbus scale) to the observed data for Aug. 18, 1969.

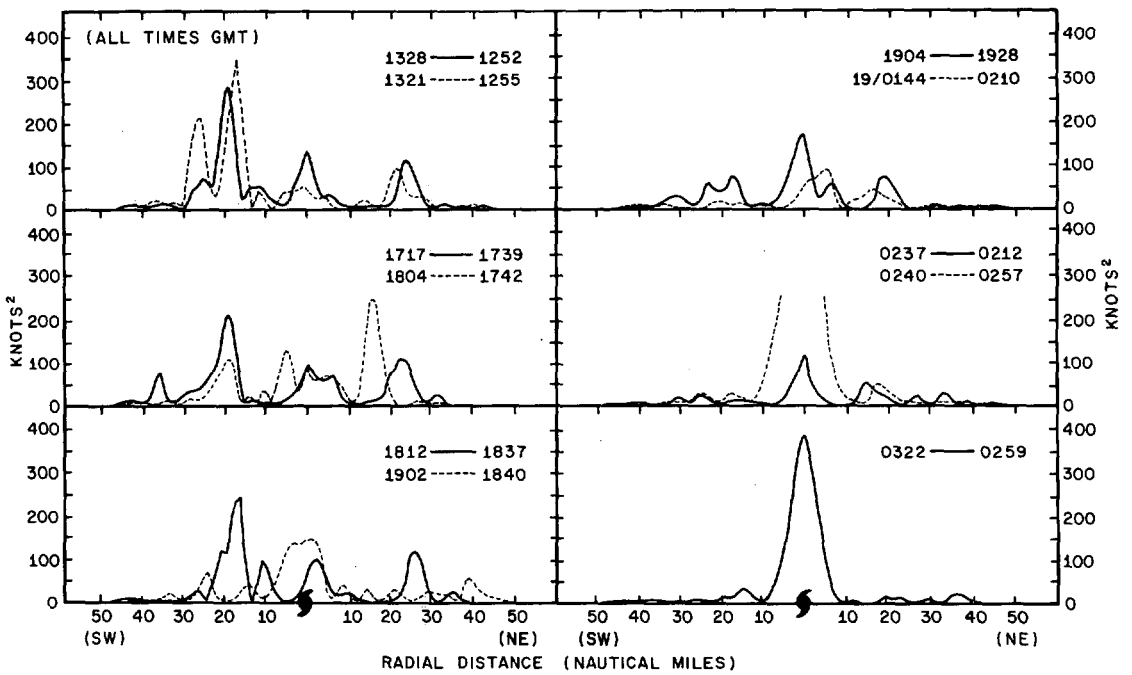

FIGURE 8.—Same as figure 7 for band filter E (≈ rainband scale).

time period are approximately 300, 500, and 650 kt², respectively, for the right side of the storm. These results indicate that an enhancement of the small-scale features is occurring during the period of the decrease in the longer wavelengths since filter A contains filter B and filter B contains filter C.

The kinetic energy associated with the cumulonimbus scale (band filter D) indicates that the southwest and northwest quadrants (only the southwest and northeast quadrants are illustrated) are the most active for this scale throughout the period of the experiment (fig. 7). Except for some enhancement in the southeast quadrant, there seem to be no large changes in this quantity through the time of the third seeding. However, a significant decrease then occurs reaching a minimum of activity near 0200 GMT on August 19. An increase is then noted through the end of the monitoring period. It is also interesting to note that the most active region for this scale is in the area immediately downstream from the seeding area (northwest and southwest quadrants), while the least active areas are behind and to the right of the storm center. However, it should be pointed out that these

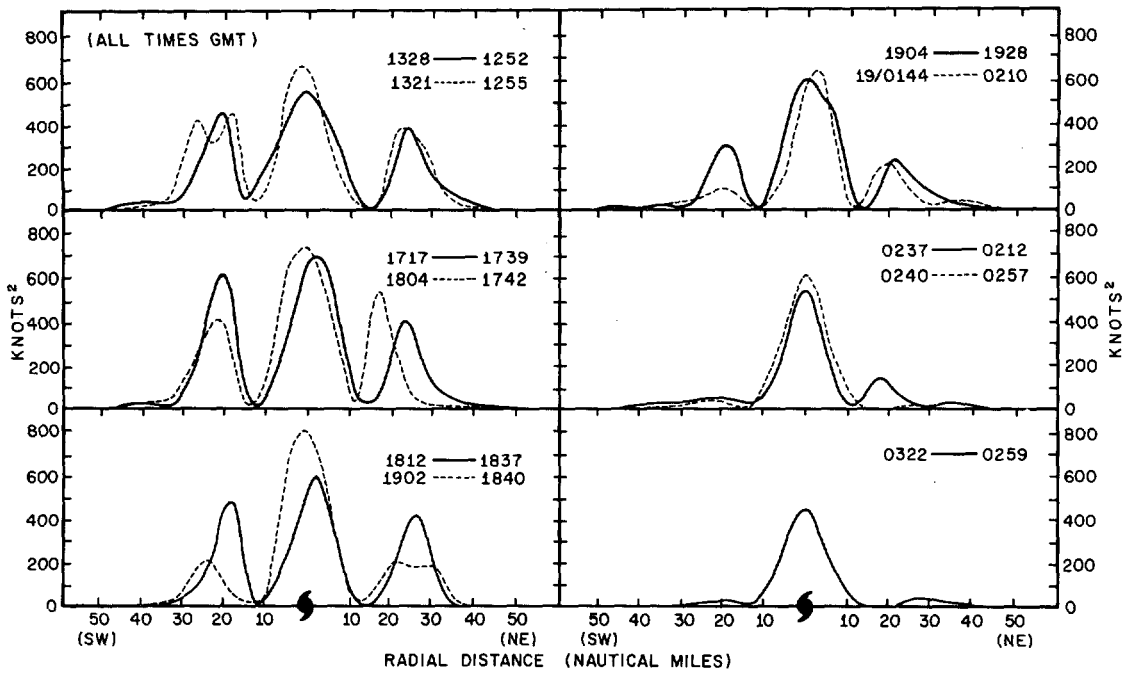

FIGURE 9.—Same as figure 7 for band filter F (≈ eyewall scale).

areas behind and to the right of the storm center are quite active prior to the first seeding, and the degree of activity does not change markedly until the time of the third seeding.

The response for the intermediate wavelengths (approximately rainband scale) indicates an increase in the northeast quadrant through the time of the third seeding and then considerable dampening for all quadrants (fig. 8) through the end of the monitoring period. Again, prior to the time of this general decrease, the most active areas for these scales are ahead and to the left of the storm center (northwest and southwest quadrants).

The response associated with the slightly longer wavelengths (approximately eyewall scale) shows increases in nearly all quadrants prior to the third seeding (fig. 9). Also, the decrease in the eye diameter during this period is noted, which agrees with the radar structure as depicted in Black et al. (1970). Probably the most significant feature of this figure is the dramatic decrease in the eyewall response after the third seeding. This response is almost nonexistent near the end of the monitoring period. This same effect appears in the northwest and southeast quadrants (not illustrated). Note also that the kinetic energy associated with this scale is generally twice as large as for the intermediate (rainband) scale and more than an order of magnitude larger than for the cumulonimbus scale.

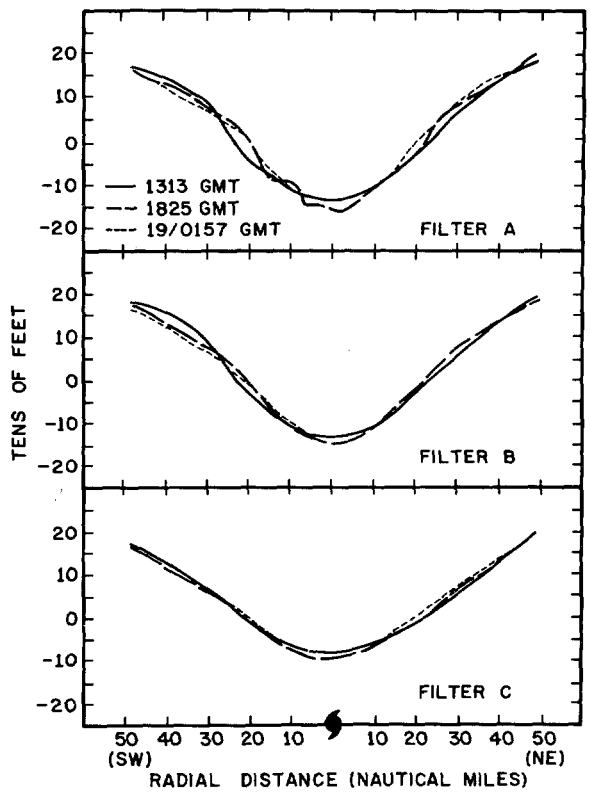

FIGURE 10.—D-value profiles for hurricane Debbie obtained by application of filters A, B, and C for the periods of before, during, and after the seeding events on Aug. 18, 1969.

Pressure

The filtered D-values show small changes in the large-scale features of the pressure field during the period of the modification experiment (fig. 10). The profiles resulting from application of filters A and B indicate a significant reduction in the pressure gradient on the southwest side of the storm during the experiment. The pressure profile for the northeast or right side of the storm indicates little change during this same period. The minimum value obtained from all three filters indicates a small decrease in pressure during the seeding, but the value recorded approximately 4 hr after the final seeding period is nearly identical to that recorded prior to any seeding. The cumulonimbus-scale features (fig. 11) exhibit large horizontal variability in time and space. However, the

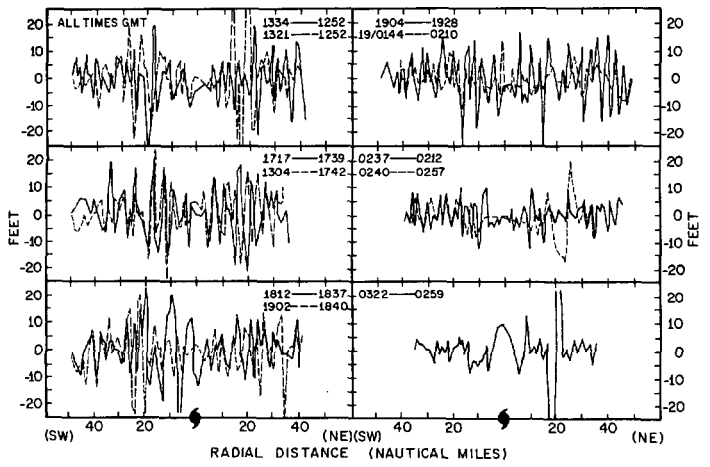

FIGURE 11.—D-value profiles for hurricane Debbie resulting from application of band filter D (≈ cumulonimbus scale) to the observed data for Aug. 18, 1969.

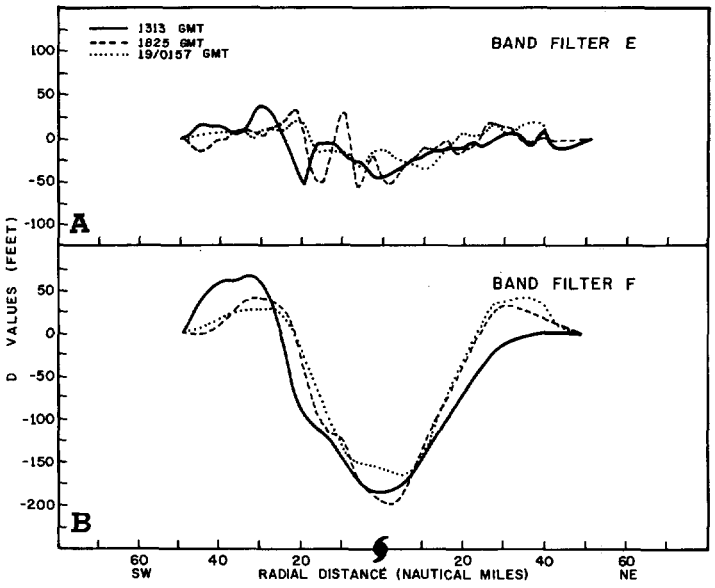

FIGURE 12.—Same as figure 11 for (A) band filter E (≈ rainband scale) and (B) band filter F (≈ eyewall scale).

dominant feature in this time sequence of profiles appears to be the decrease in the magnitude of these band-filtered D-values by the end of the seeding period. This reduction averages more than 50 percent over the horizontal distance depicted in these profiles.

The band-filtered D-value profiles for the rainband scale (filter E) also exhibit this reduction in pressure gradient, especially on the left or southwest side of the storm (fig. 12A). Again, the magnitude of these values decreases by as much as 50 percent, with almost none of the change taking place prior to the time of the third seeding run.

The band-filtered D value for the eyewall scale (≈50 n.mi.) shows a net reduction in the minimum value and the maximum value on the left side of the storm (fig. 12B). However, the right side shows an increased maximum value and gradient. In contrast to the results obtained for the cumulonimbus and rainband scales, most of the net change occurs prior to the time of the third seeding run.

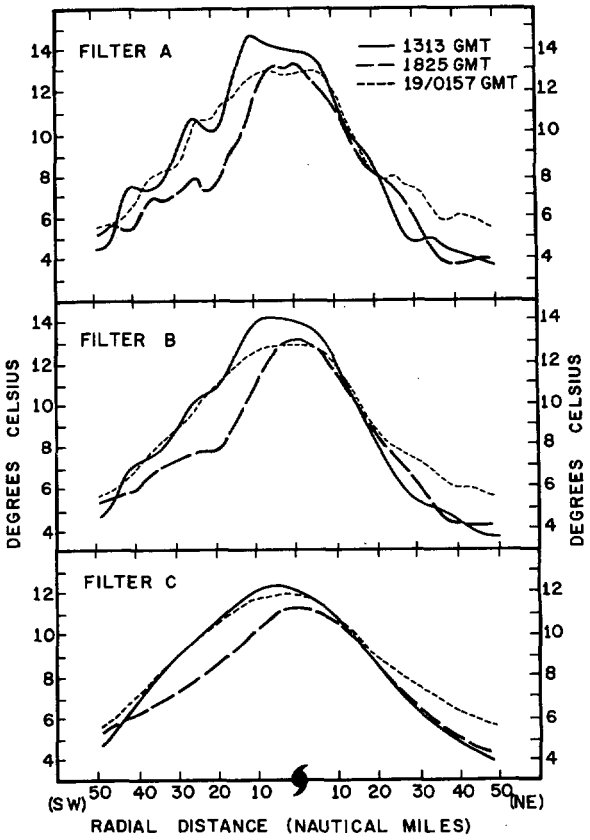

FIGURE 13.—Temperature profiles for hurricane Debbie obtained by application of filters A, B, and C for the periods of before, during, and after the seeding events on Aug. 18, 1969.

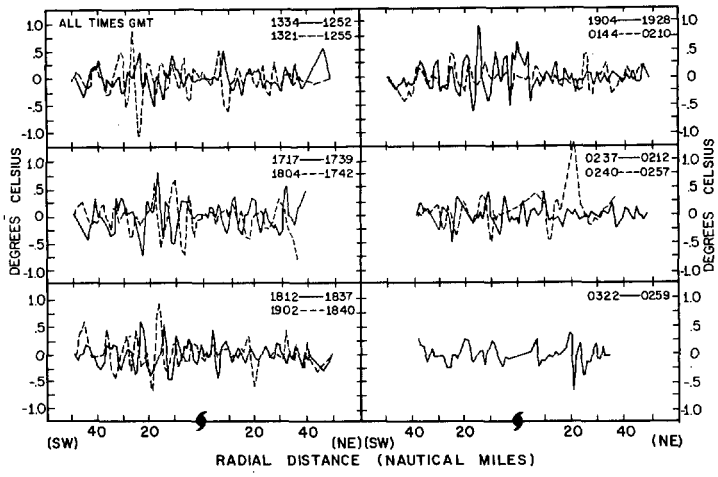

FIGURE 14.—Temperature profiles for hurricane Debbie resulting from application of band filter D (≈ cumulonimbus scale) to the observed data for Aug. 18, 1969.

Temperature

The filtered temperature profiles (fig. 13) show a net reduction in the maximum temperatures from prior to seeding until 4 hr after the final seeding event. Also shown is a significant change in the temperature field on the southwest side of the storm from prior to seeding until after the third seeding (1313–1825 GMT). However, the temperature field shows little change on the northeast side for the same period of time. By the end of the seeding operation, the thermal structure on the southwest side of the storm has returned to a state similar to that ob-

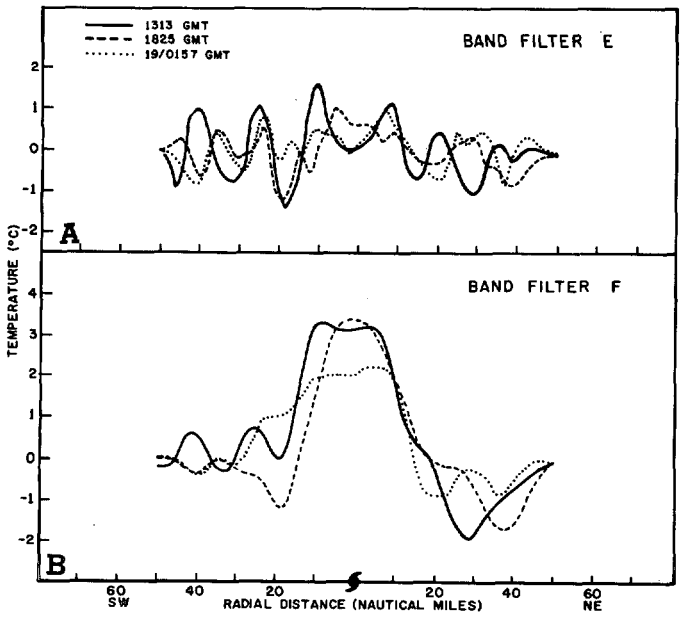

FIGURE 15.—Same as figure 14 for (A) band filter E (≈ rainband scale) and (B) band filter F (≈ eyewall scale).

served prior to the first seeding event (except for the eye and eyewall region). However, a significant change has taken place on the northeast side of the storm where the temperature increased by approximately 2°C in the outer regions after the third seeding. This change occurs in the longer wavelengths as is evidenced by the fact that nearly the same change is shown for the value obtained by application of filter C as compared to that obtained by application of filter A. It is also observed that most of the temperature reduction taking place over the central region occurs in the shorter wavelengths.

The time sequence of temperature profiles obtained by application of band filter D (cumulonimbus scale) indicates a significant reduction in the magnitude of these values after the third seeding event (fig. 14). This of course corresponds favorably to the same feature observed in the pressure profiles. The range of these values before the first seeding until after the third seeding is approximately ± 1°C. The last two profiles shown for this day and location show maximum values to be generally less than ± 0.5°C. Again, as in the case for the pressure profiles, the southwest side appears to be more active than the right side of the storm for this scale of motion.

The rainband-scale (band filter E) temperature profiles show maximum values to be about 1.5 times greater than those associated with the cumulonimbus scale (fig. 15A). Of particular significance again is the reduction in the amplitude of the temperature profile that occurs during the period of the modification experiment. The eyewall-scale (band filter F) temperature profiles also indicated that a reduction in amplitude occurs with the passage of time. A reduction in the temperature gradient in the eyewall region (approximately 15 to 30 n.mi. from the storm center) for this scale of motion is also noted. The temperature reduction over the central region exceeds 1°C for this scale, indicating that the reduction of temperature noted over the central regions in figure 13 was primarily concentrated in the eyewall scale.

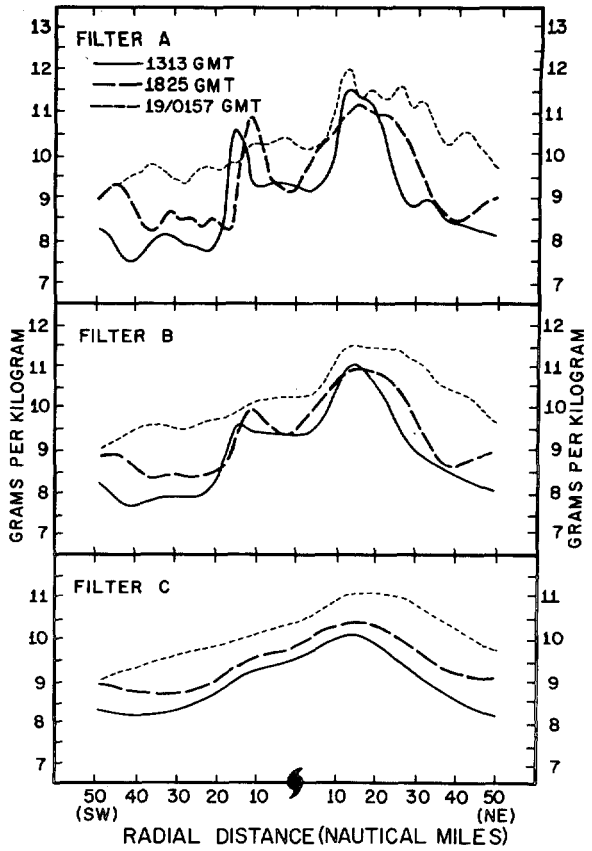

FIGURE 16.—Mixing ratio profiles for hurricane Debbie obtained by application of filters A, B, and C for the periods before, during, and after the seeding events on Aug. 18, 1969.

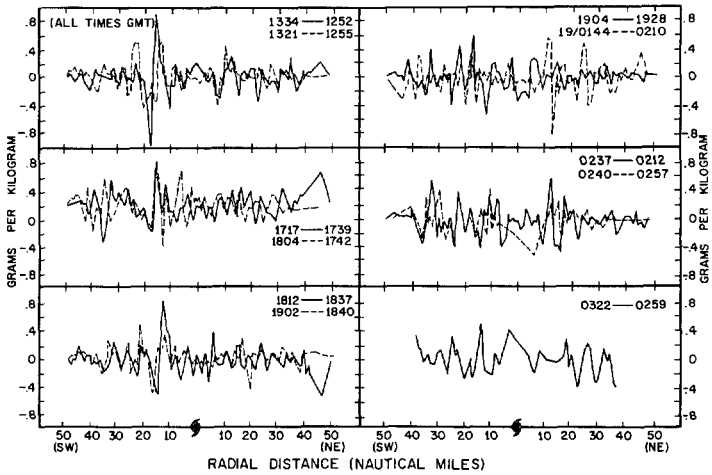

FIGURE 17.—Mixing ratio profiles for hurricane Debbie resulting from application of band filter D (≈ cumulonimbus scale) to the observed data for Aug. 18, 1969.

Moisture

The eye and eyewall region are prominent in the moisture field prior to the first seeding run as illustrated in figure 16 (filter A). That is, the eyewall region shows a relative maximum moisture content with a distinct minimum present over the interior portion of the eye. These features remain prominent throughout the time of the third seeding. However, the region of maximum mixing ratio on the northeast side of the storm has started to enlarge by 1825 GMT, and the moisture gradient has

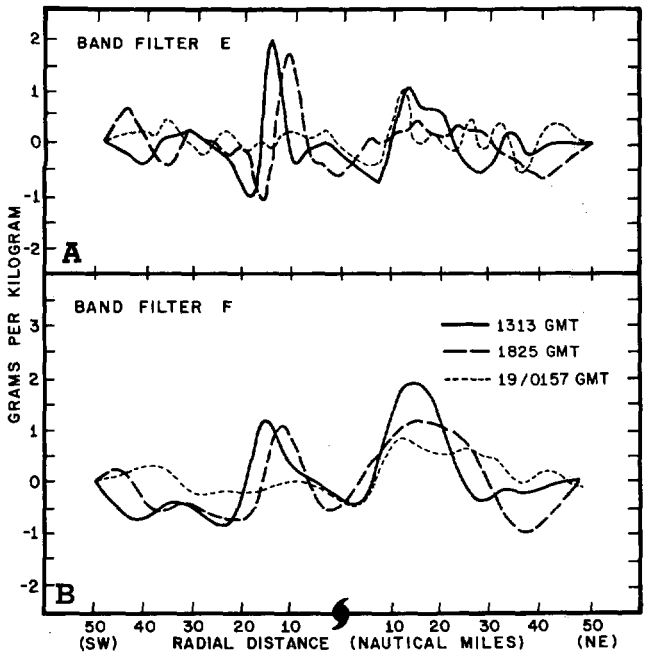

FIGURE 18.—Same as figure 17 for (A) band filter E (≈ rainband scale) and (B) band filter F (≈ eyewall scale).

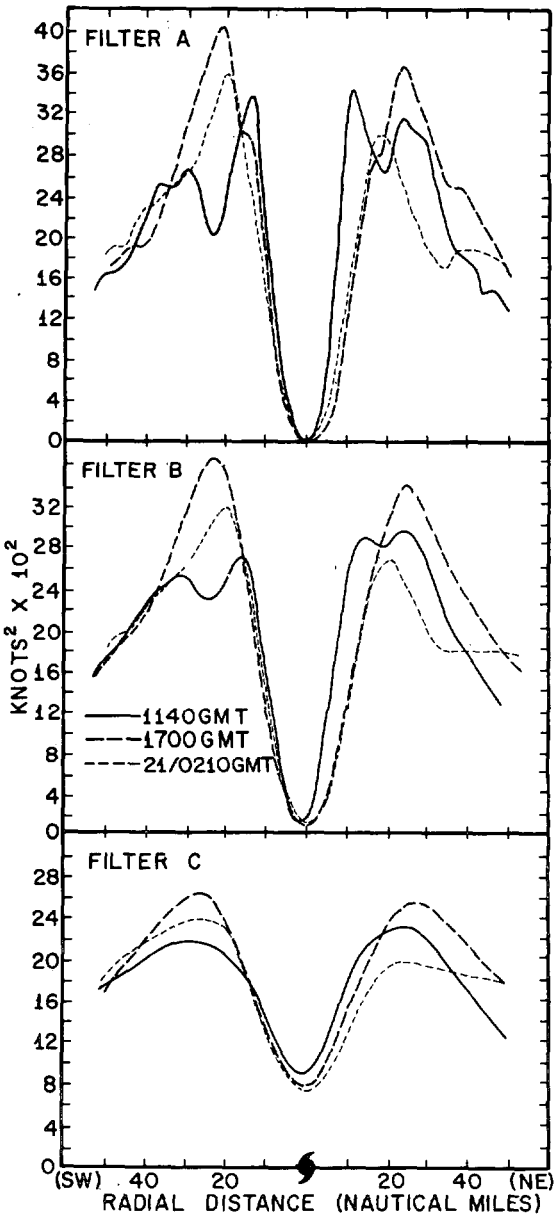

FIGURE 19.—Kinetic energy profiles for the left and right (SW–NE) sides of hurricane Debbie, obtained by application of filters A, B, and C to the observed data for Aug. 20, 1969.

decreased. The prominent regions of maximum values associated with the eyewall at 1313 GMT have nearly dissipated by 0157 GMT on August 19 (filter A). The maximum moisture values continue to be located on the right side of the storm, but the moisture has been diffused over a much larger area. The moisture profiles associated with filters B and C also indicate an increase in moisture for the entire area monitored. This increase seems to be concentrated in the longer wavelength features with average values rising by 1–1.5 g/kg over the entire area within 50 n.mi. of the storm center. A significant portion of this increase occurs prior to the time of the third seeding, especially in the outer regions monitored. However, as is the case for other parameters, the greatest portion of this change takes place after the third seeding event.

The cumulonimbus scale (band filter D) mixing ratio field (fig. 17) does not exhibit the major reduction in amplitude with time that is noted for the previously discussed parameters. However, there are a few areas where significant reductions in the extreme values are noted, particularly on the southwest side of the storm. The most prominent of these areas is the one located between 10 and 20 n.mi. left of the storm center, which persists as an identifiable feature through more than the first 6 hr of the monitoring period. The rainband-scale (band filter E) mixing ratio profiles (fig. 18A) show a major decrease in the magnitude of the values during the monitoring period, particularly on the southwest side of the storm. The resulting values are less than 0.5 g/kg by the end of the monitoring period for this area. Most of this change takes place after the time of the third seeding run. The northeast section does not show as large a net change, but in contrast to the southwest side, a major reduction occurs by the time of the intermediate pass shown, and the magnitude of the values appears to be on the increase by the end of the monitoring period. The large-scale features (band filter F) exhibit nearly the same characteristic as is observed for the rainband scale (fig. 18B). However, the values for the northeast side apparently continue to decrease through the end of the monitoring period.

5. ANALYSIS OF HURRICANE DEBBIE AUGUST 20, 1969

The method of analysis described in section 2 is also applied to data collected in hurricane Debbie on Aug. 20, 1969. This is the scheme used in the previous section, and the same parameters are investigated. The same form of data is used as for section 4 except that these data were collected on Aug. 20, 1969. More data were obtained during the August 20 operation than during the August 18 experiment, and the seeding operation began approximately 2 hr earlier than on the 18th. These differences

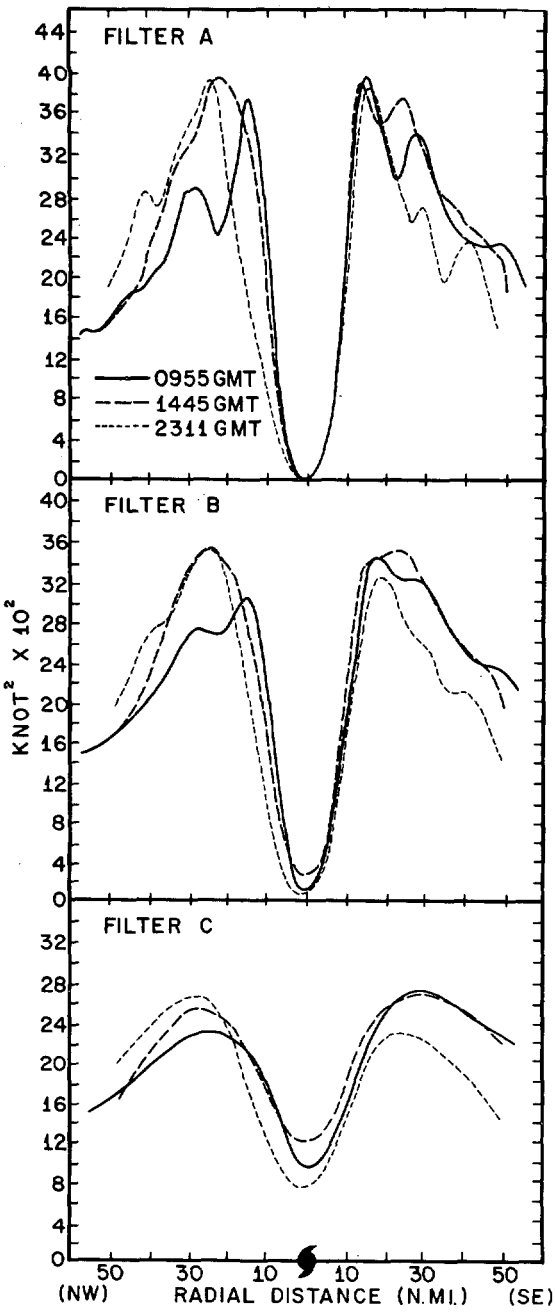

FIGURE 20.—Same as figure 19 for the front and rear (NW–SW) portions of the storm.

are primarily a result of the fact that the storm was nea r the base of operations on August 20 than it was on August 18 (fig. 1).

Kinetic Energy

The kinetic energy profiles obtained by applying filters A, B, and C to the observed data are shown in figures 19 and 20. The double maxima structure is evident in all quadrants obtained prior to the seeding runs as depicted in the profiles obtained by application of filter A. The prominence of this double structure is reduced considerably by the time of the intermediate pass and disappears by the time of the final profile shown for each quadrant. Also evident is the increase in the radius of these maxima

TABLE 2.—*Maximum (peak) values of the specific kinetic energy (kt^2) and percent changes for each quadrant in hurricane Debbie on Aug. 20, 1969**

Filter	Obs. time (GMT) (SW–NE/SE–NW)	Quadrant				Net
		SW	NE	SE	NW	
A	(1) 1140/0955	3374	3448	3931	3755	3931
	(2) 1700/1445	4069	3637	3863	3912	4069
	(3) 0210/2311	3576	2959	3822	3902	3902
	% change (1) to (2)	+20.59	+5.48	−1.72	+4.18	+3.51
	% change (2) to (3)	−12.11	−18.64	−1.06	−0.25	−4.10
	% change (1) to (3)	+5.98	−14.18	−2.77	+3.91	−0.73
B	(1) 1140/0955	2929	2691	3378	3033	3378
	(2) 1700/1445	3611	3335	3452	3495	3611
	(3) 0210/2311	3170	2666	3268	3521	3521
	% change (1) to (2)	+23.28	+23.93	+2.19	+15.23	+6.89
	% change (2) to (3)	−12.21	−20.05	−5.33	+0.74	−2.49
	% change (1) to (3)	+8.22	−0.92	−3.25	+16.08	+4.23
C	(1) 1140/0955	2317	2162	2699	2300	2699
	(2) 1700/1445	2603	2498	2720	2550	2720
	(3) 0210/2311	2368	1973	2306	2660	2660
	% change (1) to (2)	+12.34	±15.54	+0.77	+10.86	+0.77
	% change (2) to (3)	−9.02	−21.01	−15.22	+4.31	−2.20
	% change (1) to (3)	+2.20	−8.74	−14.56	+15.65	−1.44

*These values were obtained by application of filters A, B, and C and are given by quadrant as well as the net change regardless of quadrant.

in the northeast and southwest quadrants by more than 10 n.mi. between 1140 and 1700 GMT, and then slight decreases by the time of the pass at 0210 on August 21. The change in the location of these maxima is not nearly as great for the northwest and southeast quadrants.

The kinetic energy increases significantly in the northeast and southwest quadrants during the period from 1140 (prior to seeding) to 1700 GMT (after the third seeding) as indicated in table 2. This increase is 20.59 and 5.48 percent for the southwest and northeast quadrants, respectively, for filter A, 23.28 and 23.93 percent for filter B, and 12.34 and 15.54 percent for filter C. The changes in the southeast and northwest quadrants for this period are considerably less. However, the increase in the northwest quadrant is significant, being 4.18, 15.23, and 10.86 percent for filters A, B, and C, respectively. This set of numbers indicates that most of this change takes place in the longer and intermediate wavelengths since filter A contains filter B, and filter B contains filter C. A major decrease of approximately 20 percent and 10–12 percent occurs between 1700 GMT on August 20 and 0210 GMT on August 21 for all three filtered quantities in the northeast and southwest quadrants, respectively. The net result is an overall decrease in the northeast quadrant of 14, 1, and 9 percent for filters A, B, and C, respectively, while a net increase of 6, 8, and 2 percent for the same respective filtered quantities is noted for the southwest quadrant. There is a general reduction in the rear (southeast) portions of the storm and an increase in the front (northwest) portions. The rate of increase is much larger during the period from 0955 to 1445 GMT than from 1445 until 2311 GMT. Also, the kinetic energy increases at larger radial distances from the storm center in two quadrants (northwest and southwest), and the same trend appears to be taking place in the northeast quadrant.

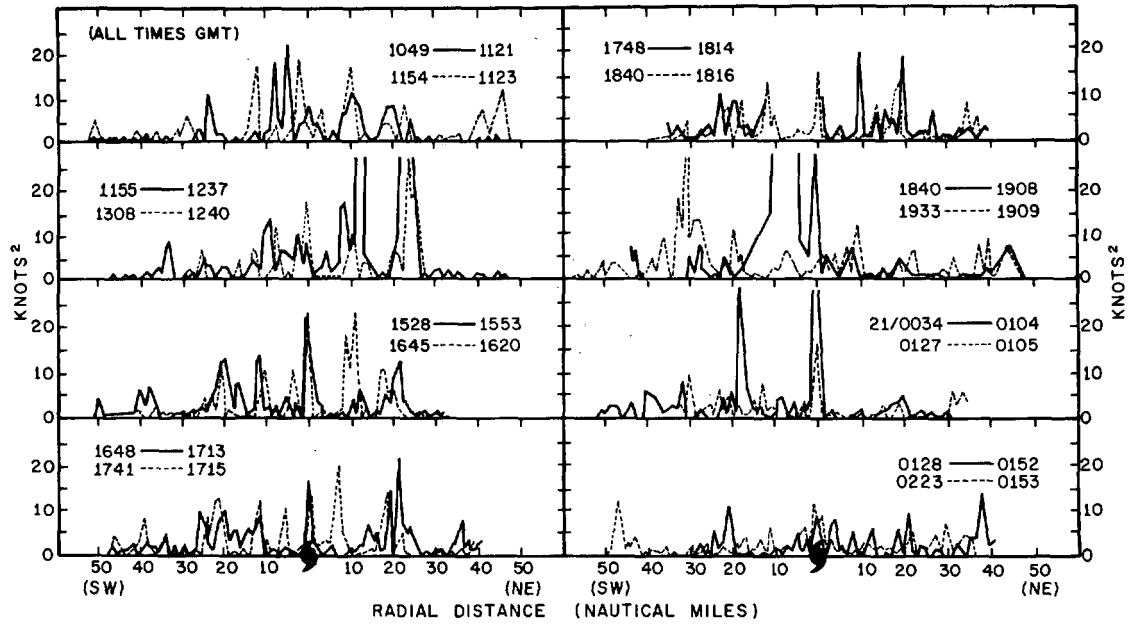

FIGURE 21.—Kinetic energy profiles for the left and right (SW–NE) sides of hurricane Debbie resulting from application of band filter D (≈ cumulonimbus scale) to the observed data for Aug. 20, 1969.

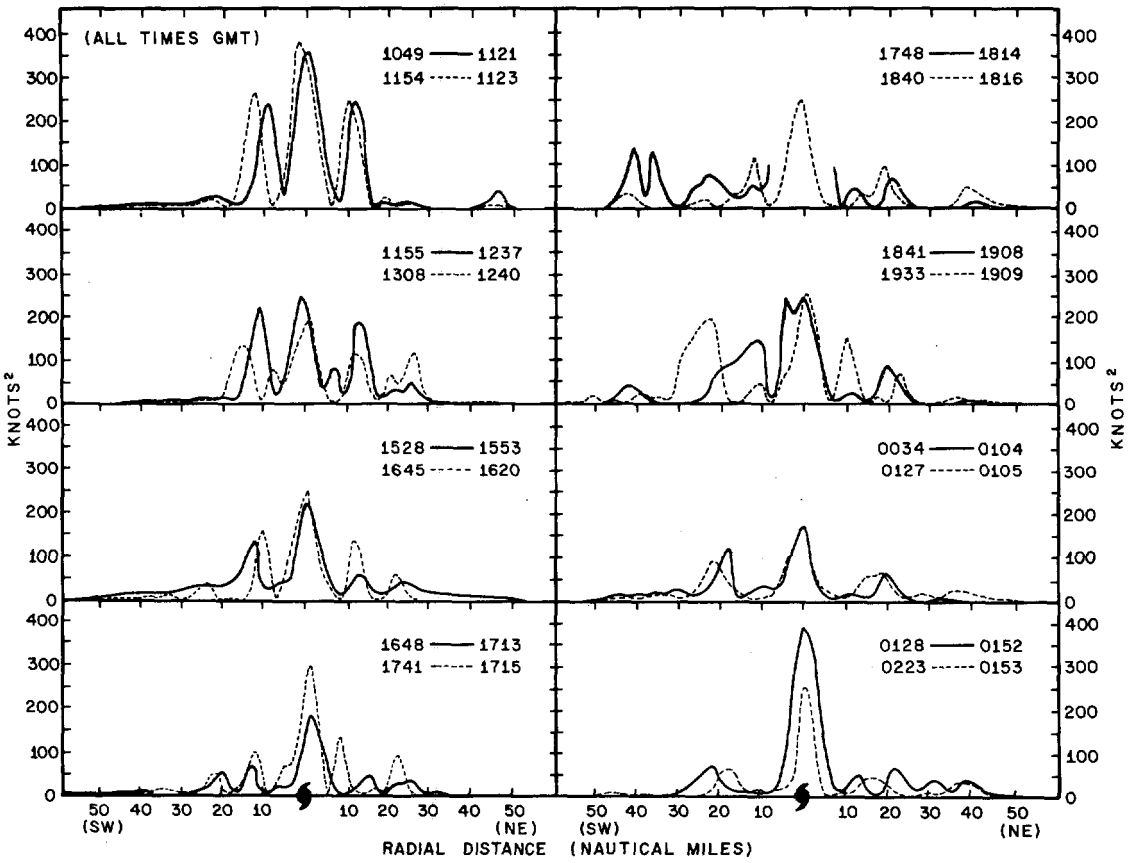

FIGURE 22.—Same as figure 21 for band filter E (≈ rainband scale).

The kinetic energy profiles associated with the cumulonimbus scale (band filter D) are shown in figure 21. This scale shows a considerable enhancement in the northeast quadrant almost immediately after the first seeding run (1155–1237 GMT). The pass made just after the second seeding run was along the direction of storm motion. The response for the cumulonimbus scale increases considerably in the northwest quadrant (not illustrated) during the period shortly after the second seeding event (1429–1456 GMT). A similar sequence of events is noted for the northeast quadrant after the third seeding. During this same period, the level of activity for this scale seems to be on the increase in the southwest quadrant. This activity reaches its peak near the end of the seeding period and

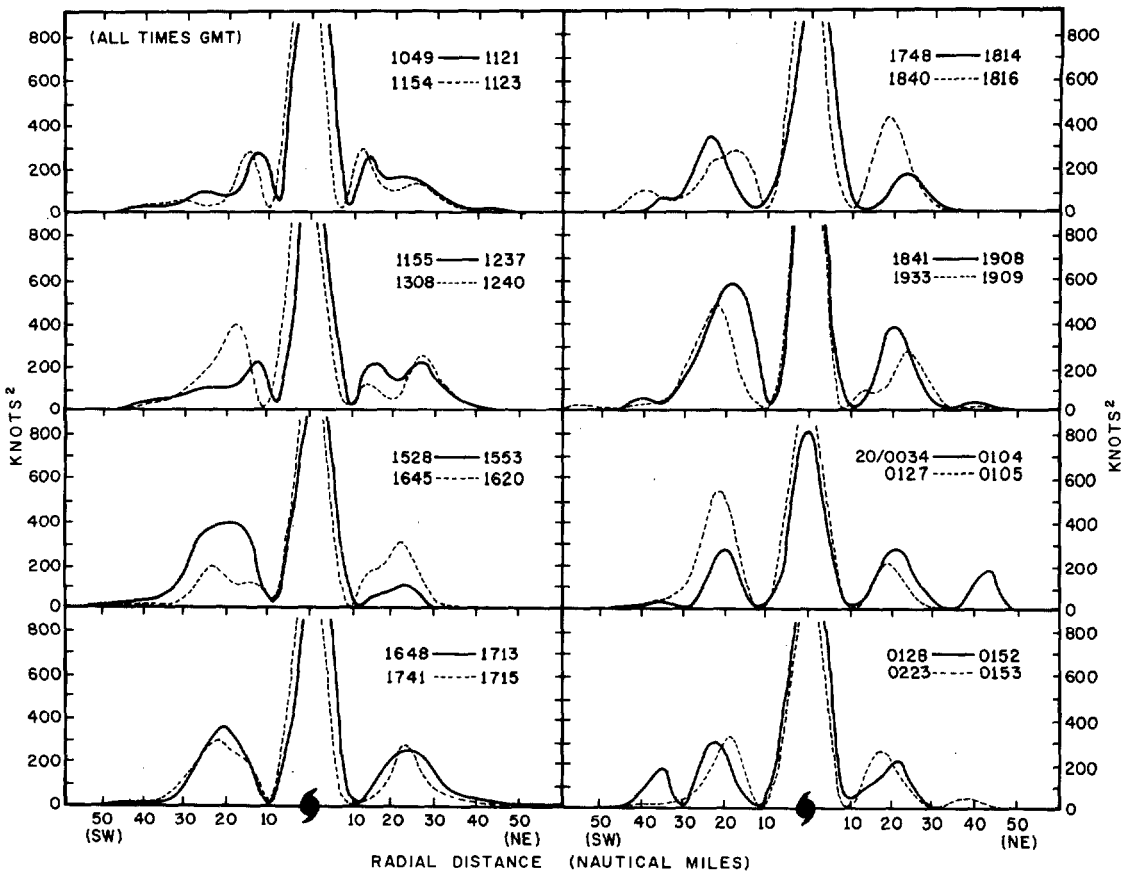

FIGURE 23.—Same as figure 21 for band filter F (≈ eyewall scale).

subsides through the end of the monitoring period. The level of activity for this scale in the northeast quadrant apparently reaches its peak earlier and then decreases nearly through the end of the monitoring period. However, the final two passes through this area, which occur some 5–6 hr after the final seeding run, indicate that the level of activity is increasing. These same profiles for the northwest and southeast quadrants covering the period of some 3–4 hr after the final seeding period indicate a high level of activity in the southeast quadrant for this scale, but with almost no response in the northwest quadrant.

The kinetic energy profiles associated with the rainband scale (band filter E) show the magnitude of the maximum value (ignoring the central values) decreasing through most of the seeding period in all quadrants (fig. 22). This decline seems to be steady through the first 6 hr of the operation, fluctuates somewhat during the period between the fourth and fifth seeding events, and then decreases again through the end of the monitoring period. The magnitude of the maximum kinetic energy value located outside the eye decreases by approximately 72, 69, 50, and 14 percent for the northeast, southwest, northwest, and southeast quadrants, respectively, for the period from prior to seeding until well after the final seeding event.

The kinetic energy profiles associated with the eyewall scale of motion (band filter F) are shown in figure 23. Prior to the time of the first seeding, the maximum kinetic energy outside the eye is relatively low. In fact, these values are only about one half of what were observed on August 18 (fig. 9). These values fluctuate considerably, but generally increase through the period of the fourth seeding and then decrease. The final result is that these values at the end of the monitoring period are nearly the same as those obtained prior to the first seeding run.

Pressure

The minimum value of the filtered D-values shows that an increase occurs between the time of the third seeding and the final monitoring pass of the day (fig. 24). Approximately one-half of this increase takes place in the long wavelengths with most of the remainder occurring in the rainband- to eyewall-scale of motion. Although the central pressure is steady through the first 6 hr of the experiment for the sum of the long and intermediate wavelengths (filters A and B), a decrease is noted for the long-wavelength features (filter C). This, of course, implies that an increase in pressure must be occurring in the intermediate wavelengths.

The cumulonimbus-scale D-value profiles (band filter D) generally show an increase in the magnitude of the horizontal variations after the first seeding (fig. 25). This parameter generally remains active through the seeding period and then dampens considerably by the end of the monitoring period. The maximum values at the end of the monitoring period are approximately 50 percent smaller than those generally observed during the seeding operation.

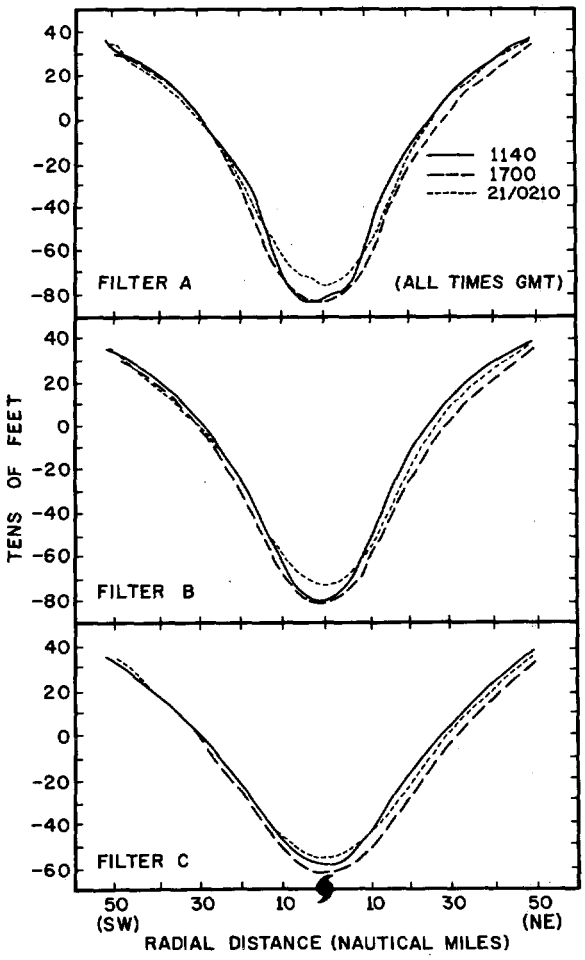

FIGURE 24.—D-value profiles for hurricane Debbie obtained by application of filters A, B, and C for the periods of before, during, and after the seeding events on Aug. 20, 1969.

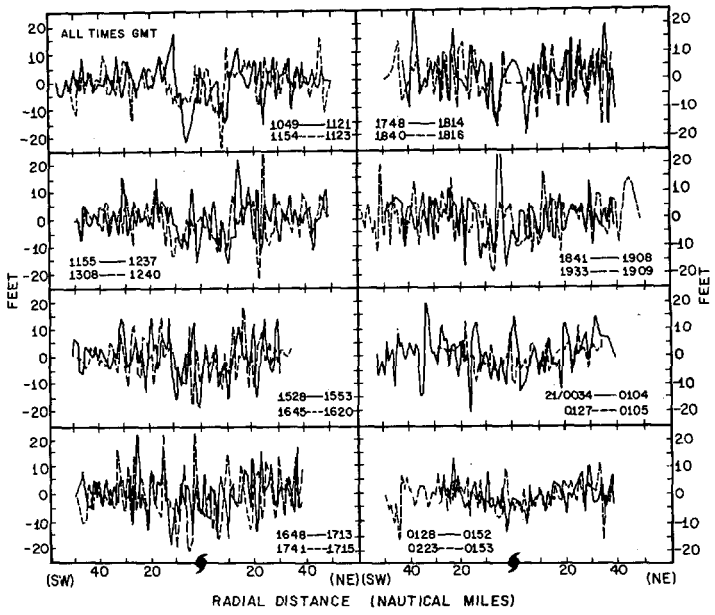

FIGURE 25.—D-value profiles for hurricane Debbie resulting from application of band filter D (≈ cumulonimbus scale) to the observed data for Aug. 20, 1969.

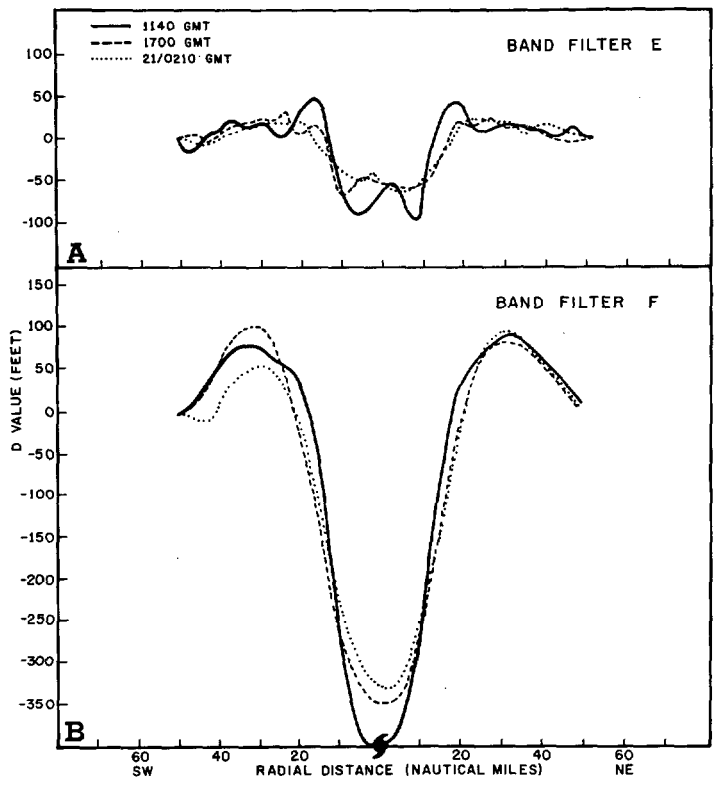

FIGURE 26.—Same as figure 25 for (A) band filter E (≈ rainband scale) and (B) band filter F (≈ eyewall scale).

The rainband-scale D-value profiles (band filter E) show a distinct decrease in the pressure gradients, particularly in the eyewall region (fig. 26A). Most of this pressure change occurs before the fourth seeding period. However, the final profile shown is much smoother than either of the two recorded earlier. Also, the maximum amplitude of the curve obtained on the last monitoring pass is 40 percent smaller than that recorded prior to seeding.

The eyewall-scale D-value profiles (band filter F) also exhibit a decrease in amplitude and pressure gradient in the eyewall region during the seeding operation. Again, a major portion of this change takes place before the fourth seeding, but a significant amount of this change occurs between the time of the fourth seeding and the final monitoring pass.

Temperature

The filtered temperature profiles (fig. 27) show that large changes occur during the seeding operation. The maximum temperature observed in the central regions of the storm shows a steady decrease with time, especially for the short and intermediate wavelengths (filters A and B). However, the major portion of the reduction that occurs in the longer wavelengths (filter C) comes after the time of the third seeding. This reduction of temperature in the longer wavelengths during the latter portion of the monitoring period accounts for most of the change in maximum temperature depicted in the illustrations for filters A and B. These results imply that a possible sequence of events occurs where the changes first appear in the shorter wavelength features and then progress through the longer wavelengths. Of particular interest in

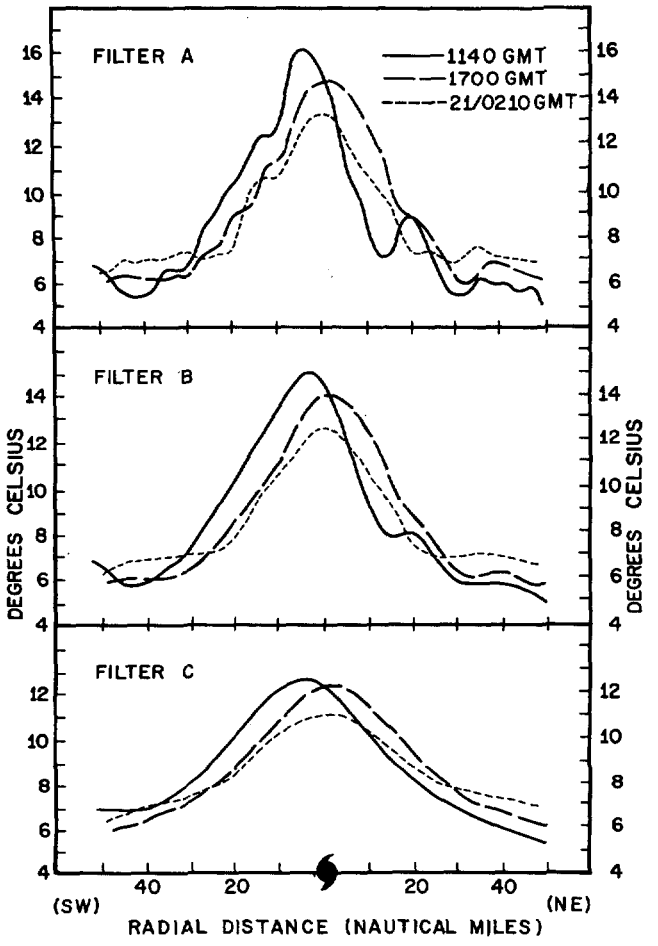

FIGURE 27.—Temperature profiles for hurricane Debbie obtained by application of filters A, B, and C for the periods of before, during, and after the seeding events on Aug. 20, 1969.

this set of profiles is the reduction of temperature gradient that occurs. This feature is particularly evident in the eyewall region on the northeast side of the storm and is present in all three filtered quantities. The temperature profiles also become smoother during the experiment as illustrated by the disappearance of the secondary temperature maximum located on the northeast side of the storm. During this same time interval, the temperature increases in the outer regions of the storm covered by the monitoring pattern.

The time sequence of temperature profiles representing the cumulonimbus scale (band filter D) indicates that a considerable reduction in the maximum value occurs during the monitoring period (fig. 28). In fact, the maximum amplitude of the curves for the temperatures recorded at the end of the monitoring period is less than one-half of that observed prior to the first seeding. The largest portion of this reduction appears to occur during the early portion of the monitoring period. However, there is a general trend of maximum values decreasing through most of the period of the experiment. The northeast and southwest sides of the storm appear to be about equally active for this scale of motion during most of the monitoring period.

The temperature profiles representing the rainband scale (band filter E) also show a considerable reduction in amplitude occurring during the period of the experiment (fig. 29A). Most of this change occurs prior to the time of the fourth seeding event. The reduction in the temperature gradient for this scale of motion is large, particularly in the northeast quadrant. The eyewall-scale temperature profiles (band filter F) indicate this same general trend (fig. 29B). The central value decreases by 2°C during the monitoring period with three-fourths of this change taking place prior to the time of the fourth seeding. During the same period, the minimum temperatures increase by approximately 1°C. These two changes resulted in a major reduction of the hurricane-scale temperature gradient.

Moisture

The double eye structure present during the early portions of the modification experiment in hurricane Debbie on Aug. 20, 1969, is evident in the moisture field analysis for this time (fig. 30). This feature is present prior to the first seeding (1140 GMT) but becomes considerably less distinct by 1700 GMT. However, some semblance of this structure remains throughout the monitoring period, especially in the profiles obtained by application of filter A. Note also that the minimum central value increases during the period of the experiment. This feature is prominent in both sets of profiles obtained through use of filters A and B. During this same period, the total amount of moisture is increasing over the central and southwestern portions of the storm. This is especially true for the longer wavelengths, where the value increases by approximately 1.0–1.5 g/kg.

The cumulonimbus-scale mixing ratio profiles (band filter D) show a trend toward a slight decrease with the passing of time after the first seeding period (not illustrated). The minimum average amplitude is recorded some 4–5 hr after the final seeding event; larger amplitudes are noted for the final two passes through the area.

The mixing ratio profiles associated with the rainband scale (band filter E) are depicted in figure 31A. The average amplitude of the profile for 21/0210 GMT is approximately one-half that recorded prior to the first seeding event. The eyewall-scale mixing ratio profiles (band filter F) show a trend toward less horizontal variation during the period of the experiment. This feature is particularly evident over the central regions. The minimum central value increases by approximately 2 g/kg during this period while the value in the eyewall remains nearly constant.

6. COMPARISON OF ANALYSIS RESULTS WITH SEEDING HYPOTHESES I AND II

Seeding hypothesis I is vague and difficult to evaluate in terms of the data collected. Also, the experiment as conducted was not exactly as proposed in seeding hypothesis I. That is, the seeding was not confined to the eyewall region, but extends some distance outward from the eyewall. No direct measurements were made of the change in the supercooled water-to-ice ratio in the seeded

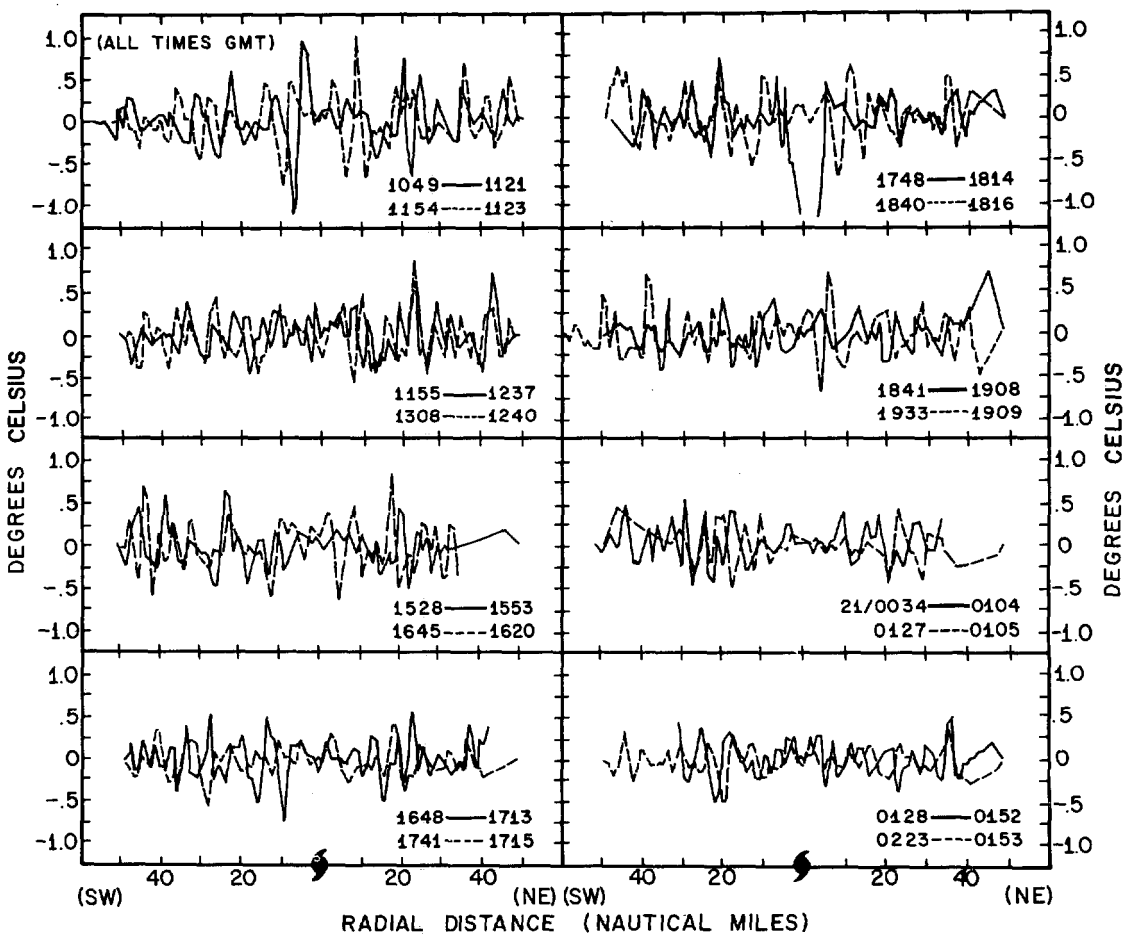

FIGURE 28.—Temperature profiles for hurricane Debbie resulting from application of band filter D (≈ cumulonimbus scale) to the observed data for Aug. 20, 1969.

regions of hurricane Debbie. However, temperature, wind, and pressure measurements were made, which give an indication of what probably occurs in the areas of supercooled water.

Hypothesis I basically suggests that a reduction in the maximum temperature and pressure gradients should result, along with a corresponding reduction in the maximum wind speeds. These conditions are all observed to occur in the analysis previously discussed. However, other changes take place that do not correspond favorably with hypothesis I. For example, the reduction in temperature gradients is hypothesized to be the result of increasing the temperature on the exterior edge of the maximum temperature gradient. In actuality, this reduction in temperature gradient was more a result of the decrease in temperatures over the central region, whereas the temperature in the maximum wind speed region shows only small net changes from prior to the first seeding run until after the final monitoring pass through the storm during the experiment.

Seeding hypothesis II is more explicit, and the experiment as carried out in hurricane Debbie conforms much more to the procedure proposed by hypothesis II than hypothesis I. Hypothesis II calls for stimulating convection at radii from the region of maximum wind speeds outward. This region of increased convection then competes with the eyewall region for the inflowing air at low levels. The expected results are reduction in the

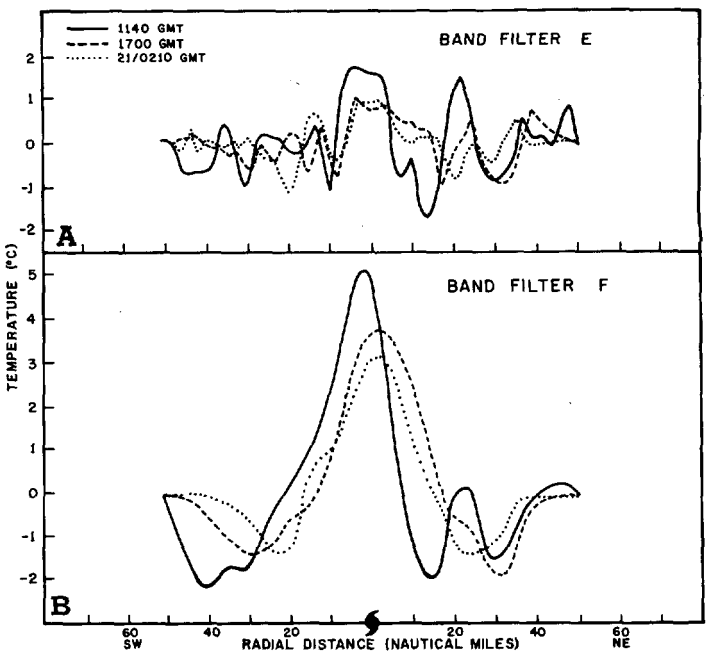

FIGURE 29.—Same as figure 28 for (A) band filter E (≈ rainband scale) and (B) band filter F (≈ eyewall scale).

prominence of the old eyewall region, reduced temperature and pressure gradients in the old eyewall region, and a resulting decrease in the maximum wind speeds. The results of the experiment in hurricane Debbie on Aug. 18,

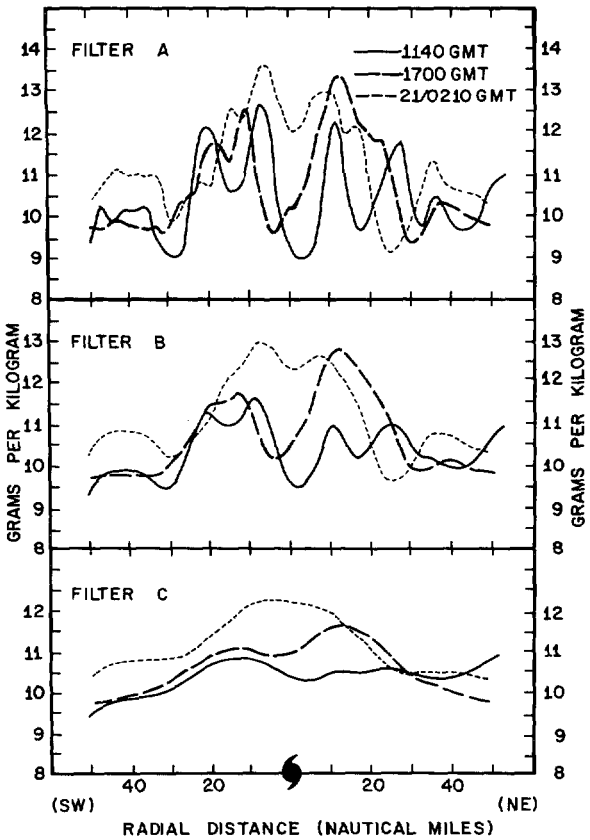

FIGURE 30.—Mixing ratio profiles for hurricane Debbie obtained by application of filters A, B, and C for the periods of before, during, and after the seeding events on Aug. 20, 1969.

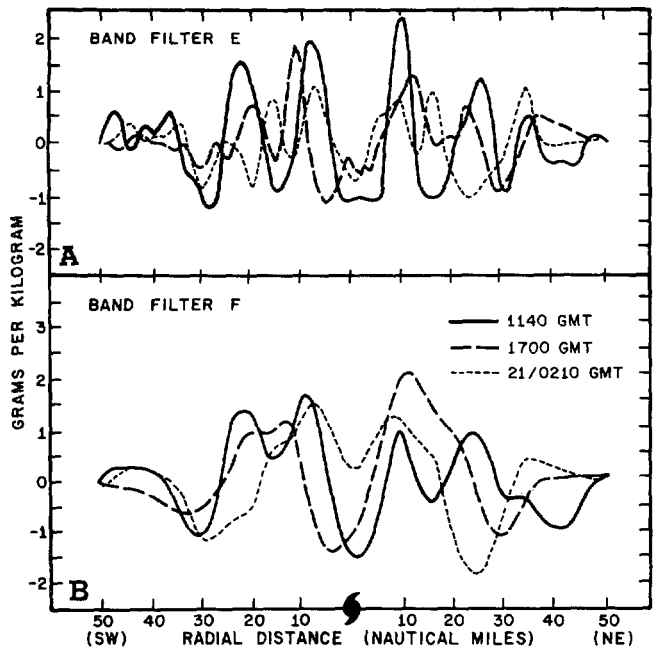

FIGURE 31.—Same as figure 30 for (A) band filter E (≈ rainband scale) and band filter F (≈ eyewall scale).

1969, strongly suggest that all of these events occurred at least through the period of the first three seeding runs. That is, the reduction in temperature over the central region and slight increases at larger radii indicate that some portion of the inflowing air at low levels, which normally serves to drive the storm's transverse circulation through the eyewall region, is being intercepted at larger radii. Also, there is some evidence of increased convection during the early portion of the seeding operation. After the time of the third seeding, the small- and intermediate-scale features become much more diffuse, suggesting a possible merging of the smaller scale features.

The reduction in the large-scale feature, which occurred on Aug. 18, and the increase, which occurred on Aug. 20, 1969, in hurricane Debbie, were not predicted by either hypothesis I or II. In fact, calculations of the decrease in maximum winds to be expected from the seeding experiment are of the order of 10 to 15 percent. These results imply that the seeding effects were being superimposed on a large-scale change that was occurring naturally.

7. SUMMARY AND CONCLUSIONS

The research reported on in this paper is concerned with three basic problems. The first is to develop consistent analysis techniques that can be used to evaluate the structure and intensity of tropical storms as well as changes in the state of the storm with time. Particular attention is placed on the cumulonimbus, rainband, and eyewall scales of motion. The techniques should also provide an objective means of comparing the analyzed results from one time to another and from one storm to another where particular interest is placed on the high energy portion of the storm. The second goal is to apply these techniques to the data collected during modification experiments conducted in hurricane Debbie on Aug. 18 and 20, 1969, and evaluate changes that occurred in the storm structure. Also, we wish to determine what portion of these changes could reasonably be attributed to the seeding experiments. The third goal is to use the results of the analyses of hurricane Debbie to develop a more explicit and detailed seeding hypothesis, which could be used in the statistical evaluation of future modification experiments. That is, to determine a set or sequence of events that would occur with a seeded storm but would have a low probability of occurring under natural conditions.

Hurricane Debbie was seeded five times on both Aug. 18 and 20, 1969. The maximum wind speed prior to the seeding events was nearly the same for both days. However, the structure of the storm was somewhat different; a single eyewall structure was present on August 18 (figs. 5, 6), while a double eyewall structure was initially present on August 20 (figs. 19, 20). Many of the changes that occurred prior to, during, and after the seeding events were different for the 2 days. However, many common features were also observed to occur during this same period.

The kinetic energy profiles shown in figures 5 and 6 and the percentage changes listed in table 1 indicate that the maximum kinetic energy value decreases for all represented wavelengths from prior to seeding until the end of the

monitoring missions on August 18. The net changes listed in table 1 show that a major portion of the reduction associated with the intermediate and shorter wavelengths occurs after the period of the third seeding, while that associated with the longer wavelengths (filter C) occurs prior to the time of the third seeding event. In fact, if one computes the change in kinetic energy from the last column in table 1, values of -341, -479, and -640 kt^2 are obtained for filters A, B, and C, respectively, for the change between observation times (1) and (2). Since filter A contains B and filter B contains C, these results indicate that a major reduction is taking place in the longer wavelengths and that the intermediate and shorter wavelengths are actually enhanced during this period. However, if these same quantities are computed for the time period from time (2) to time (3) (after the third seeding until near the end of the monitoring period), values of -1369, -942, and -280 kt^2 are obtained for filters A, B, and C, respectively. These values indicate that the long-wave feature continues to decrease in intensity during this time period, but at a much slower rate than earlier. Also, the intermediate and shorter wavelength features, which are enhanced prior to the time of the third seeding, undergo a dramatic reduction during this time period. These characteristics are further illustrated in figures 7 and 8, which show a time series of band-filtered kinetic energy profiles. A general enhancement is shown for most of the scales of motion represented through the time of the third seeding, and then a dramatic decrease is shown through the end of the monitoring period.

The resulting changes of kinetic energy obtained for, Aug. 20, 1969, show some different characteristics. The changes in kinetic energy for the last column in table 2 are 138, 233, and 21 kt^2 for filters A, B, and C, respectively for the period from time (1) to time (2) (prior to the first seeding until after the third seeding event). These results indicate an increase in kinetic energy for the sum of all the wavelengths represented. However, most of this increase was confined to features of eyewall scale or larger for this time period. The same quantities for the period from after the third seeding until the end of the monitoring period are -167, -90, and -60 kt^2 for filters A, B, and C, respectively. These results imply a reduction at all wavelengths represented, since the value for filter A is a larger negative number than for C. These results are also illustrated in figures 21 and 22 where we see a distinct increase in the eyewall scale through the periods of the first three or four seedings and then a decrease. During this same period, the rainband scale (fig. 22) appeared to be decreasing steadily through the period of the modification experiment. At the same time, the cumulonimbus scale shows an overall enhancement through the period of the third or fourth seeding events and then a considerable decrease.

A summary of the kinetic energy analyses for these two seeding experiments indicates that on August 18 a large-scale decrease, which cannot reasonably be attributed to the seeding operation, occurs prior to and during most of the monitoring period. Likewise, a large-scale increase in intensity takes place on August 20 during the early portion of the seeding operation. A major portion of this increase is apparently associated with the change from a double to a single eyewall structure and, also, could not reasonably be attributed to the seeding operation. However, a significant decrease occurs in these longer wavelength features after the time of the third or fourth seeding. In general, the results for the smaller and intermediate scale features show some enhancement during the early portion of the seeding operations on both days, and then a distinct decrease through the end of the monitoring periods.

The analyses of the pressure fields for August 18 show a general decrease in the pressure gradient associated with the large-scale feature (fig. 10) occurring during the seeding experiment. Most of this change takes place prior to the time of the third seeding, a condition which was also observed in the kinetic energy analyses. However, the minimum central pressure shows little change between the times of the first and last passes illustrated. The pressure profiles associated with cumulonimbus (fig. 11), rainband, and eyewall (fig. 12) scales also exhibit characteristics similar to those of the kinetic energy analyses. That is, these scales show a general decrease in the magnitudes of their extreme values, with most of the change taking place after the time of the third seeding period.

The analyses of pressure for August 20 also show a general decrease in the pressure gradient for the long-wave features (fig. 24) occurring basically after the time of the third seeding event. The cumulonimbus-scale pressure profiles (fig. 25) indicate a reduction in the magnitudes of the extreme values near the end of the seeding operation. The rainband and eyewall scales on August 20 also show distinct pressure gradient decreases occurring during the seeding operation.

The temperature analyses for these same periods exhibit characteristics almost identical to those depicted in the pressure analyses; that is, a general reduction in the temperature gradients for nearly all scales represented during the period of the modification experiment. In addition, temperature decreases and increases are shown to occur over the central and outer regions of the storm, respectively (figs. 13, 27). This feature is generally reflected in the corresponding pressure profiles, but it is not as readily discernible due to the scale of the plotted graphs.

The moisture analyses also exhibit the same general characteristics as the pressure and temperature fields. However, in addition to these characteristics, the moisture level shows a distinct and significant increase occurring on both days over most of the high energy portion of the storm during the period of the modification experiments (figs. 16, 30). Most of this increase is associated with the longer wavelength feature. Also, the distinct dry region over the central portions of the storm, which is present during the early passes, becomes almost nonexistent by the end of the monitoring period. The eyewall regions, quite distinct in the moisture analyses for the early passes, are also nearly eliminated (figs. 18, 31).

The following general observations can be made concerning the overall changes in structure that occurred during the seeding experiments conducted in hurricane Debbie on Aug. 18 and 20, 1969. First, a general reduction in the amplitudes and gradients of most of the parameters analyzed occurred on both days for scales of motion of eyewall scale or smaller during the period of the experiments. This reduction generally occurred after the time of the third or fourth seeding; that is, some 4–6 hr after the first seeding run. There appeared to be a temporary enhancement of the smaller scale features during the early portions of the seeding operation, but the evidence for this condition was generally not as strong as for the decrease for these same scales during the latter portions of the experiment periods. The moisture level also rose over most of the high energy portion of the storm, and in general the structure of the storm became more symmetrical for nearly all parameters during the modification experiments. These similarities in changes for the two seeding cases (August 18 and 20) occurred despite the fact that the longwave features were acting in opposite directions for the 18th as compared to those for August 20. These results offer strong evidence supporting the basic seeding hypothesis discussed in section 2 of this paper. They are the basis for the more explicit hypothesis which is proposed in the next subsection.

Proposed Seeding Hypothesis

The hypothesis proposed here is basically an elaboration of hypothesis II discussed in section 2. The details of this proposed hypothesis are based on the interpretation of the results obtained in the analyses described earlier and results of other seeding experiments conducted on cloudlines, individual clouds, and cloud groups. The intent is to help explain the events that may occur in a hurricane seeding operation and to propose a sequence of events that hopefully is likely to occur with a particular seeding experiment and highly unlikely to occur naturally. If successful, this hypothesis would be of considerable aid in the statistical evaluation of hurricane seeding experiments.

Hypothesis II calls for seeding from the exterior edge of the band of maximum winds radially outward for a distance of approximately 20 n.mi. The basic idea is to enhance convection at radii greater than the eyewall. The analysis results indicate that this effect probably took place during the early portions of the seeding operations on both August 18 and 20. The following sequence of events could reasonably be expected to occur. First, the individual towers or cells containing supercool water would grow; this, along with the fact that the seeding occurs in a somewhat continuous manner over a 20-n.mi. interval, would then cause the systems to merge over this region.

The fact that individual cloud systems can be caused to expand in horizontal coverage and probably merge has been amply demonstrated in project Stormfury cloudline seeding operations and by Woodley (1970) and Simpson and Woodley (1971) during experiments conducted over south Florida. The merging of these systems does not occur instantaneously. Therefore, one would expect the changes in structure resulting from seeding to progress from small-scale features to larger scales, and no major change in the mesoscale structure would be expected for the first 3–4 hr of the experiment. Large-scale filling or deepening of the storm during the first few hours of the experiment would probably dominate the early seeding effects. Large-scale changes appeared to have been taking place during the early periods of the Debbie experiments. Therefore, it is deduced that this was a natural occurrence upon which the seeding effect was being superimposed.

The strong horizontal wind components would spread the seeding agent and its effect around the high energy portion of the storm. The widespread enhanced convection would raise the moisture levels throughout the high energy portion of the storm. At the same time, the increased ascent at larger radii than the eyewall would decrease the prominence of the eyewall by competing with the eyewall for the low-level inflowing moisture-laden air. The merging of the cloud systems would also decrease the prominence of the individual cumulonimbus clouds and hurricane rainbands.

Each of these features was observed or can be implied to have occurred in Hurricane Debbie on both Aug. 18 and 20, 1969. The time periods over which these changes took place were sometimes difficult to determine primarily because of the inability to monitor seeded areas continuously. Some regions in the vicinity of the seeded areas were monitored shortly after seeding, and nearly instantaneous reaction to the seeding was apparent. Of course, the number of such cases is few, and it is difficult to state with a large degree of confidence that this short-term change was directly related to the seeding event. However, an almost instantaneous reaction to seeding agents has been observed in project Stormfury cloudline seeding experiments (fig. 1) and in numerous individual cumulus seeding experiments such as those conducted by Woodley and Simpson (1970). Woodley and Simpson found that seeded clouds grew considerably more than similar clouds that were not seeded. The growth potential was predicted through use of their cumulus cloud model. It is not unreasonable to assume that this same reaction could be expected in the hurricane environment considering the computations previously made by the author (Sheets 1969*c*) using a version of the same cloud model.

We will now enumerate the sequence of events that should occur in a hurricane seeded in a manner similar to the seeding conducted in hurricane Debbie of 1969 and having a distinct eyewall structure with an associated maximum wind speed band. This same sequence of events was observed to have actually occurred on both hurricane Debbie seeding days or at least can be implied to have occurred based on interpretation of the analyzed data.

The sequence of events and results are:

1. Enhancement of small-scale features as depicted in the wind, temperature, and pressure fields (cumulus and cumulonimbus scales) in the immediate vicinity of the seeded area, particularly beyond the eyewall region, within minutes of the actual seeding event. This reaction should occur with the first three or four seeding events (4- to 6-hr period after first seeding run).

2. Intermediate-scale features as depicted in the wind, temperature, pressure, and moisture fields (rainband and eyewall scales) remain prominent or slightly enhanced during the first three or four seeding events.

3. By the time of the third or fourth seeding event, the seeding agent and its effects are dispersed over the high energy portion of the storm with the following results, which occur and persist through the next 6- to 8-hr period (period of from 6–14 hr after the commencement of the seeding operation):

a. A general reduction in the temperature, pressure, and moisture gradients, particularly for rainband- and eyewall-scale motions with the resulting reduction in the prominence of these features.

b. A reduction in the maximum temperature values over the central regions and an increase in temperature at radii beyond the eyewall region.

c. A reduction in the original wind speed maximum associated with the eyewall resulting from the decreased angular momentum and moisture supplies to the eyewall and increased ascent of moisture laden air at larger radii.

d. A general increase in the moisture levels for the large-scale features covering the high energy portion of the hurricane.

As stated earlier, the sequence of events listed above is intended as an elaboration of hypothesis II in an effort to assist in evaluation of future seeding experiments. The list was compiled based primarily upon the analyses of two hurricane seeding experiments and knowledge gained from other seeding events and logical deductions. However, as one reviewer pointed out, it is possible that a coincidence may have occurred naturally in the two cases that has been deduced to have occurred as a result of the seeding events. It is even more likely that other events occurred due to the seeding, which were not included in the proposed sequence of events. Therefore, the proposed hypothesis is listed here merely as a plausible conjecture to guide future investigation.

The conclusions drawn above are based upon, and to be applied to, data collected in the middle and lower troposphere. However, with the vertical continuity known to exist in the hurricane (several case studies previously cited), these results should apply to most of the tropospheric portion of the hurricane.

ACKNOWLEDGMENTS

Yoshikazu Sasaki deserves considerable credit for his scientific advice, without which the research reported on in this paper would not have been completed. Considerable computer time on the University of Oklahoma IBM 360 and 1130 systems as well as the CDC 6600 and 7600 at the National Center for Atmospheric Research was also provided through his efforts.

The basis for the work presented in this paper has evolved from more than 6 yr of research effort by the author at the NOAA National Hurricane Research Laboratory (NHRL) and during a year at the University of Oklahoma under a NOAA scholarship. Scientific direction and advice have been received from R. Cecil Gentry, Harry F. Hawkins, Stanley L. Rosenthal, and Banner I. Miller during this period. Almost the entire staff of NHRL have contributed to some phase of the research effort and to preparing this paper for publication. Special thanks are also due the operational crews of the NOAA Research Flight Facility aircraft who collected the majority of the data used in this study.

REFERENCES

Black, Peter G., Senn, Harry V., and Courtright, Charles L., "Eye-Size Changes in Hurricane Debbie on 18 and 20 August 1969," *Project STORMFURY Annual Report*, **1969**, U.S. Department of Commerce and U.S. Department of the Navy, Appendix E, Washington, D.C., May **1970**, 10 pp.

Colon, Jose A., and Staff, "On the Structure of Hurricane Daisy (1958)," *Report* No. 48, *National Hurricane Research Project*, U.S. Weather Bureau, Washington, D.C., Oct. **1961**, 102 pp.

Colon, Jose A., "On the Structure of Hurricane Helene (1958)," *Report* No. 72, *National Hurricane Research Project*, U.S. Weather Bureau, Washington, D.C., Dec. **1964**, 56 pp.

Friedman, Howard A., Cicirelli, Frank S., and Freedman, William S., "The ESSA Research Flight Facilities: for Airborne Atmospheric Research," *ESSA Technical Report* ERL 126-RFF 1, Miami, Fla., Aug. **1969***a*, 89 pp.

Friedman, Howard A., Ahrens, Merlin R., and Davis, Harlan W., "The ESSA Research Flight Facility: Data Processing Procedures," *ESSA Technical Report* ERL 132-RFF 2, Miami, Fla., Nov. **1969***b*, 64 pp.

Gentry, R. Cecil, "Hurricane Debbie Modification Experiments, August, 1969," *Science*, Vol. 168, No. 3930, Apr. 24, **1970**, pp. 473–475.

Hawkins, Harry F., and Rubsam, Daryl T., "Hurricane Hilda, 1964—II. Structure and Budgets of the Hurricane on October 1, 1964," *Monthly Weather Review*, Vol. 96, No. 9, Sept. **1968**, pp. 617–636.

Jordan, Charles L., "Mean Soundings for the West Indies Area," *Journal of Meteorology*, Vol. 15, No. 1, Feb. **1958**, pp. 91–97.

La Seur, Noel E., and Hawkins, Harry F., "An Analysis of Hurricane Cleo (1958) Based on Data From Research Reconnaissance Aircraft," *Monthly Weather Review*, Vol. 91, Nos. 10–12, **1963**, pp. 694–709.

Rosenthal, Stanley L., "Numerical Experiments of Relevance to Project STORMFURY," *NOAA Technical Memorandum* ERL NHRL–95, U.S. Department of Commerce, National Hurricane Research Laboratory, Miami, Fla., Dec. **1971**, 52 pp.

Sasaki, Yoshikazu, "An Objective Analysis Based on the Variational Method," *Journal of the Meteorological Society of Japan*, Vol. 36, No. 3, Tokyo, June **1958**, pp. 77–88.

Sasaki, Yoshikazu, "Numerical Variational Method of Objective Analysis: Principle of Initialization," *Report* No. 10, University of Oklahoma Research Institute, Norman, **1968**, 21 pp.

Sasaki, Yoshikazu, "Proposed Inclusion of Time Variation Terms, Observational and Theoretical, in Numerical Variational Objective Analysis," *Journal of the Meteorological Society of Japan*, Vol. 47, No. 2, Tokyo, Apr. **1969**, pp. 115–124.

Sasaki, Yoshikazu, "Some Basic Formalisms in Numerical Variational Analysis," *Monthly Weather Review*, Vol. 98, No. 12, Dec. **1970***a*, pp. 875–883.

Sasaki, Yoshikazu, "Numerical Variational Analysis Formulated Under the Constraints as Determined by Longwave Equations and a Low-pass Filter," *Monthly Weather Review*, Vol. 98, No. 12, Dec. **1970***b*, pp. 884–898.

Sasaki, Yoshikazu, "Numerical Variational Analysis With Weak Constraint and Application to Surface Analysis of Severe Storm Gust," *Monthly Weather Review*, Vol. 98, No. 12, Dec. **1970***c*, pp. 899–910.

Sheets, Robert C., "On the Structure of Hurricane Janice, 1958," *Technical Memorandum* NHRL–76, National Hurricane Research Laboratory, U.S. Department of Commerce, Miami, Fla., Apr. **1967***a*, 38 pp.

Sheets, Robert C., "On the Structure of Hurricane Ella, 1962." *Technical Memorandum* NHRL–77, National Hurricane Research Laboratory, U.S. Department of Commerce, Miami, Fla., Apr. **1967***b*, 33 pp.

Sheets, Robert C., "The Structure of Hurricane Dora, 1964," *Technical Memorandum* NHRL 83, National Hurricane Research Laboratory, U.S. Department of Commerce, Miami, Fla., Dec. **1968**, 64 pp.

Sheets, Robert C., "Some Mean Hurricane Soundings," *Journal of Applied Meteorology*, Vol. 8, No. 1, **1969***a*, pp. 134–146.

Sheets, Robert C., "Preliminary Analysis of Cloud Physics Data Collected in Hurricane Gladys, 1968," *Project STORMFURY Annual Report* 1968, U.S. Department of Commerce and U.S. Department of the Navy, Appendix D, Washington, D.C. May **1969***b*, 11 pp.

Sheets, Robert C., "Computations of the Seedability of Clouds in a Hurricane Environment," *Project STORMFURY Annual Report 1968*, U.S. Department of Commerce and U.S. Department of the Navy, Appendix E, Washington, D.C., May **1969***c*, 5 pp.

Sheets, Robert C., "Application of Bayesian Statistics for STORMFURY Results," *Project STORMFURY Annual Report* 1969, U.S. Department of Commerce and U.S. Department of the Navy, Appendix H, Washington, D.C., May **1970**, 15 pp.

Sheets, Robert C., "Diurnal Variation in Hurricanes," *Project STORMFURY Annual Report* 1971, U.S. Department of Commerce and U.S. Department of the Navy, Appendix G, Washington, D.C., June **1972***a*, pp. 121–126.

Sheets, Robert C., "Some Statistical Characteristics of the Hurricane Eye and the Minimum Surface Pressure," *Project STORMFURY Annual Report* 1971, U.S. Department of Commerce and U.S. Department of the Navy, Appendix I, Washington, D.C., June **1972***b*, pp. 143–156.

Sheets, Robert C., "Analysis of STORMFURY Data Using the Variational Optimization Approach," *NOAA Technical Report*, ERL 264–WMPO–1, U.S. Department of Commerce, Boulder, Colo., Apr. **1973**, 92 pp.

Simpson, Joanne S., and Woodley, William L., "Seeding Cumulus in Florida: New 1970 Results," *Science*, Vol. 172, No. 3979, Apr. 9, **1971**, pp. 117–126.

Simpson, Robert H., and Malkus, Joanne S., "Experiments in Hurricane Modification," *Scientific American*, Vol. 211, No. 6, New York, N.Y., Dec. **1964**, pp. 27–37.

Wagner, K. K., "Variational Analysis Using Observational and Low-pass Filtering Constraints," Department of Meteorology, University of Oklahoma, Norman, **1971**, 39 pp. (unpublished).

Woodley, William L., "Rainfall Enhancement by Dynamic Cloud Modification," *Science*, Vol. 170, No. 3954, Oct. 9, **1970**, pp. 127–132.

[*Received February 2, 1973; revised July 13, 1973*]